The CGM around Eris at z ~2-3: A Test for Stellar Feedback, Galactic Outflows and Cold Streams

Sijing Shen
IMPS Fellow, UC Santa Cruz

Santa Cruz Galaxy Workshop   August 17th, 2012

In collaboration with: Piero Madau, Javiera Guedes, Jason X. Prochaska, James Wadsley & Lucio Mayer

Shen et al. arXiV:1205.0270

The CGM-Galaxy Interactions

The CGM-Galaxy Interactions

- Galactic outflows

- Galactic outflows observed in local starburst with v ~ hundreds km/s (e.g., Shapley+2003; Veilleux+2005; Weiner+2009)

The CGM-Galaxy Interactions

- Galactic outflows

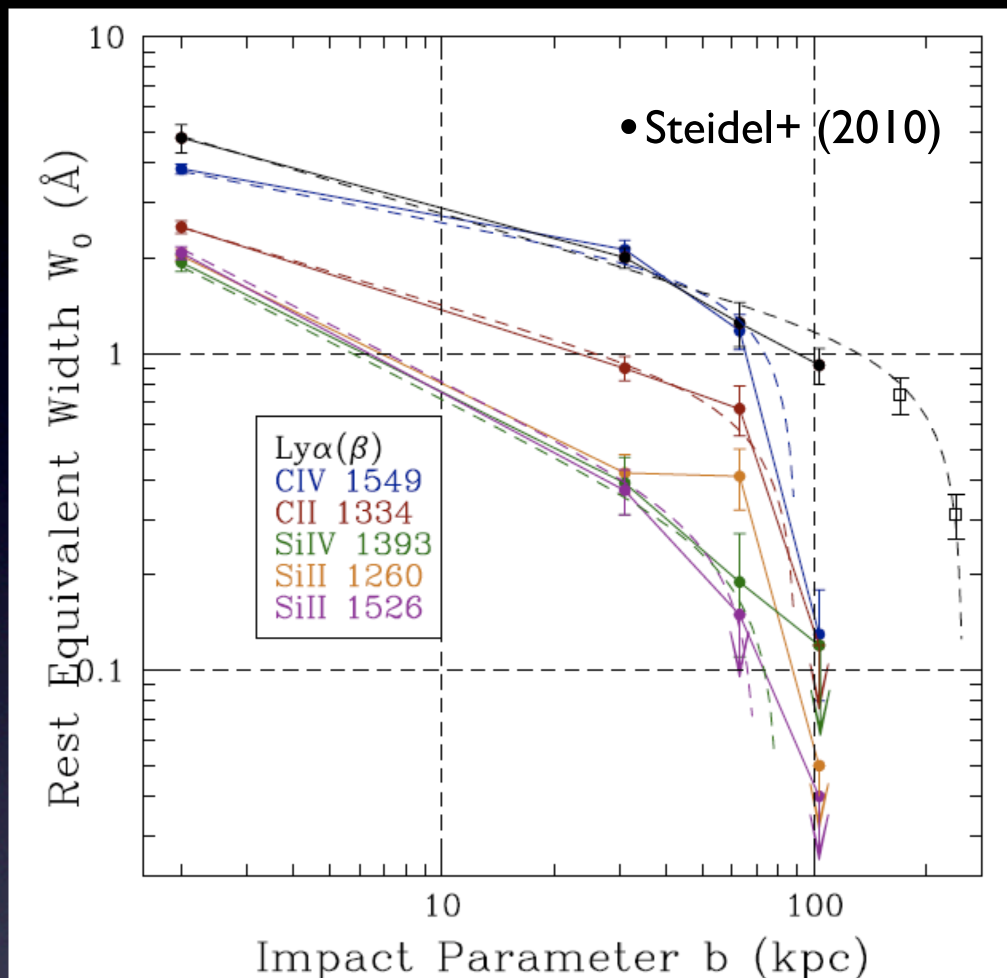

rst

- Far-UV spectra of angular pairs of galaxies/ quasar-galaxies provides detailed map of the CGM metals (e.g., Steidel+2010) and H I (e.g., Rudie+2012) at higher z

- Increasing amount of data about the CGM at low redshift (e.g., Prochaska & Hennawi 2009; Chen +2010; Crighton+2011; Prochaska+2011; Tumlinson +2012; Werk+2012)

The CGM-Galaxy Interactions

- Galactic outflows

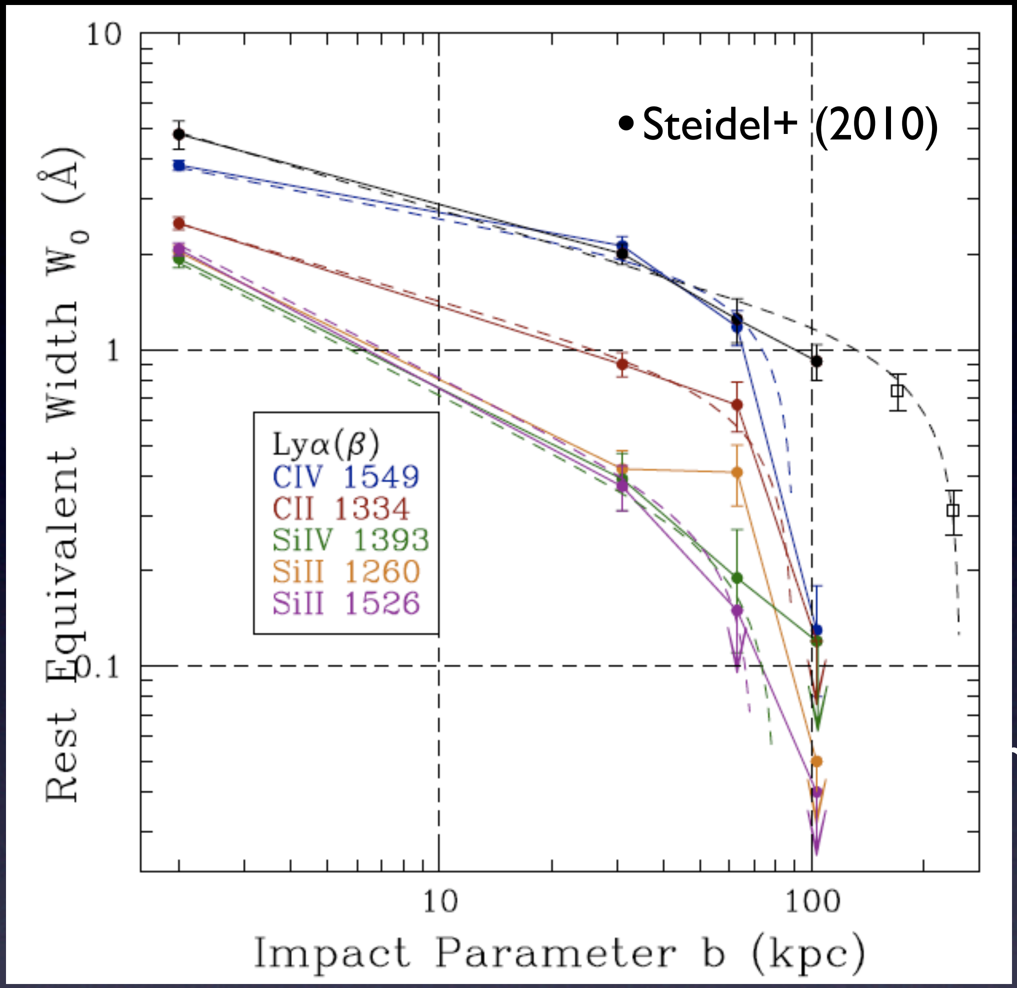

rst

Gas from IGM inflows into galactic halos

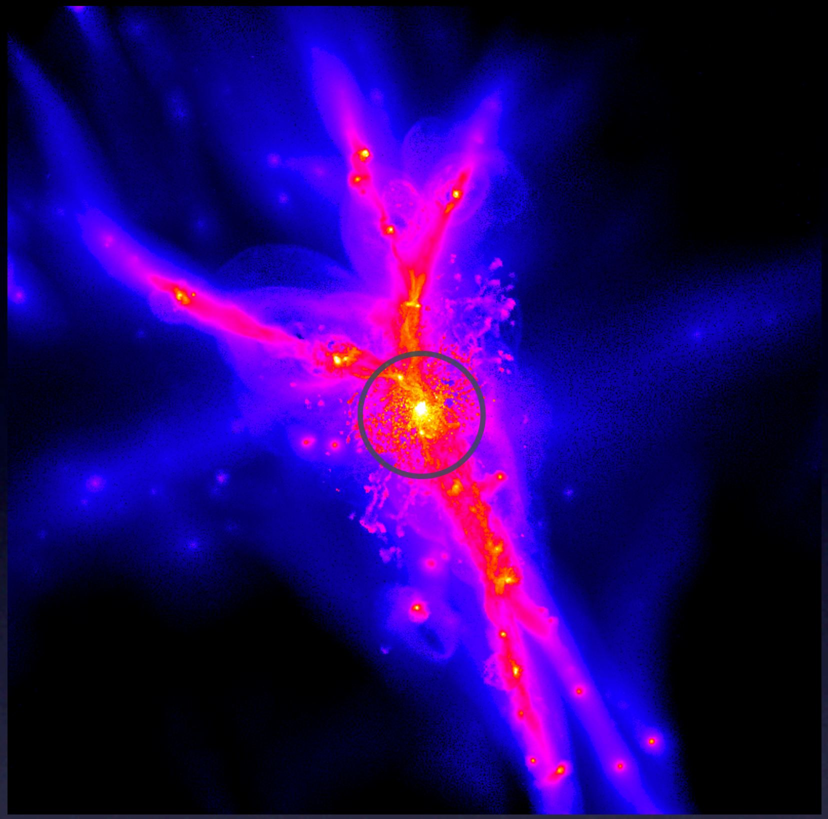

- Far-UV spectra of angular pairs of galaxies/ quasar-galaxies provides detailed map of the CGM metals (e.g., Steidel+2010) and H I (e.g., Rudie+2012) at higher z

- Increasing amount of data about the CGM at low redshift (e.g., Prochaska & Hennawi 2009; Chen +2010; Crighton+2011; Prochaska+2011; Tumlinson +2012; Werk+2012)

The CGM-Galaxy Interactions

•Galactic outflows

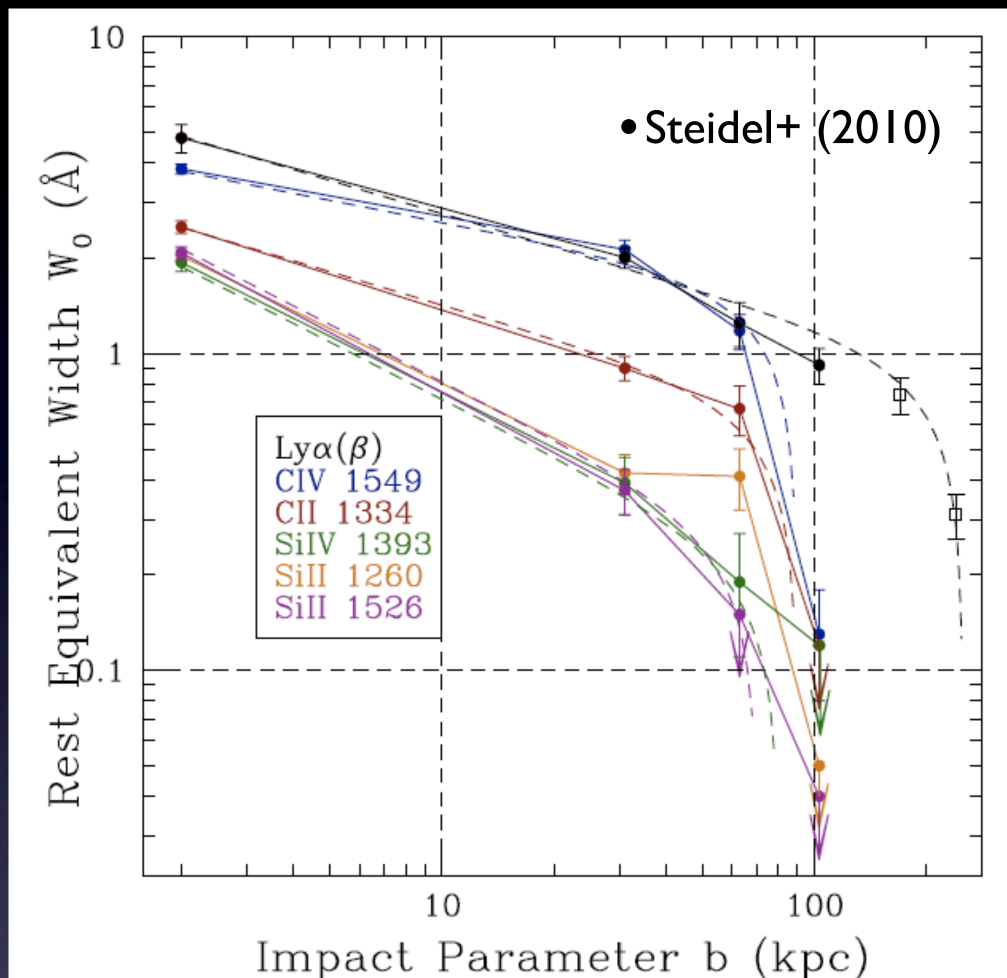

rst

•Far-UV spectra of angular pairs of galaxies/ quasar-galaxies provides detailed map of the CGM metals (e.g., Steidel+2010) and H I (e.g., Rudie+2012) at higher z

•Increasing amount of data about the CGM at low redshift (e.g., Prochaska & Hennawi 2009; Chen +2010; Crighton+2011; Prochaska+2011; Tumlinson +2012; Werk+2012)

Gas from IGM inflows into galactic halos

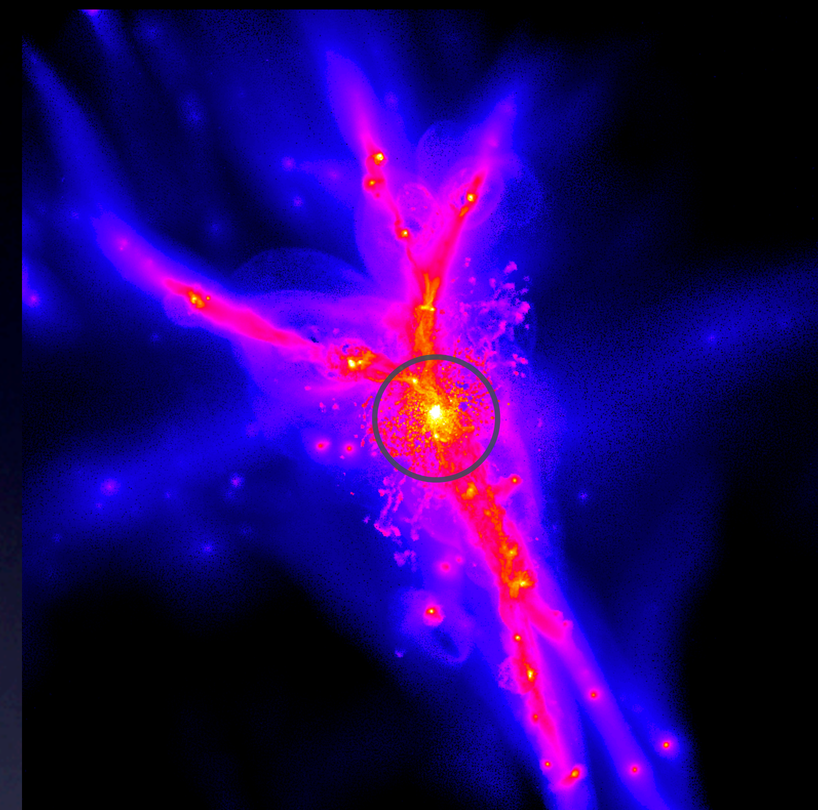

•At high z, "cold" accretion mode dominates (e.g., Kereš+ 2005, 2009; Dekel & Birnboim 2006; Ocvirk+2008)

•Prediction of cold stream detection

1) statistical prescription using cosmological volumes (e.g., Dekel+2009; van de Voort+2012) and

2) "zoom-in" simulations(e.g., Fumagalli+ 2011; Faucher-Giguère & Kereš 2011; Kimm +2011; Stewart+2011; Goerdt+ 2012)

The Eris2 Simulation

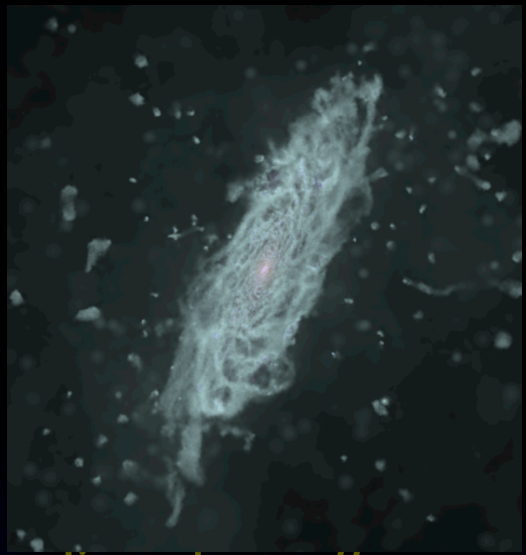

- TreeSPH code Gasoline (Wadsley et al. 2004)
- SF: $d\rho_*/dt = \varepsilon_{SF}\rho_{gas}/t_{dyn} \propto \rho_{gas}^{1.5}$ when gas has $n_H > n_{SF}$
- Blastwave feedback model for SN II (Stinson+ 2006): radiative cooling shut-off according to analytical solution from McKee & Ostriker (1977).
- Radiative cooling for H, He and metals were computed using Cloudy (Ferland+ 1998), assuming ionization equilibrium under uniform UVB (Haardt & Madau 2012)
- Turbulent diffusion model (Wadsley+ 2008; Shen+2010) to capture mixing of metals in turbulent outflows.
- Same initial set up as in Eris (Guedes+2011)

Galaxy	m_{DM} (Ms)	m_{SPH} (Ms)	ε_G (pc)	n_{SF} (cm^{-3})
Eris2	9.8×10^4	2×10^4	120	20.0

The Eris2 Simulation

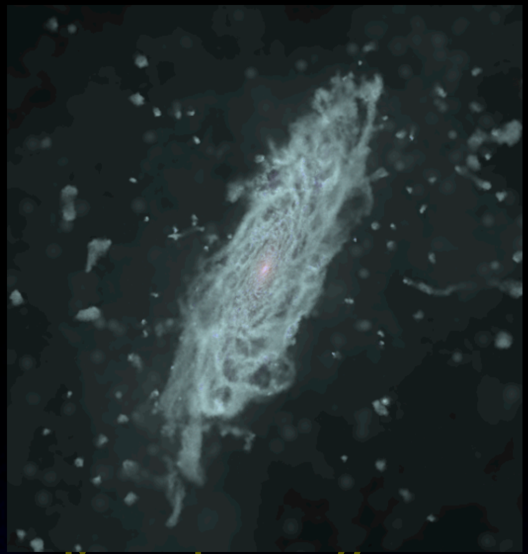

- TreeSPH code Gasoline (Wadsley et al. 2004)
- SF: $d\rho_*/dt = \varepsilon_{SF}\rho_{gas}/t_{dyn} \propto \rho_{gas}^{1.5}$ when gas has $n_H > n_{SF}$
- Blastwave feedback model for SN II (Stinson+ 2006): radiative cooling shut-off according to analytical solution from McKee & Ostriker (1977).
- Radiative cooling for H, He and metals were computed using Cloudy (Ferland+ 1998), assuming ionization equilibrium under uniform UVB (Haardt & Madau 2012)
- Turbulent diffusion model (Wadsley+ 2008; Shen+2010) to capture mixing of metals in turbulent outflows.
- Same initial set up as in Eris (Guedes+2011)

Galaxy	m_{DM} (Ms)	m_{SPH} (Ms)	ε_G (pc)	n_{SF} (cm^{-3})
Eris2	9.8×10^4	2×10^4	120	20.0

Very high resolution - 4 M particles within Rvir at z =2.8, to resolve the galaxy structure, the progenitor satellites and dwarfs

The Eris2 Simulation

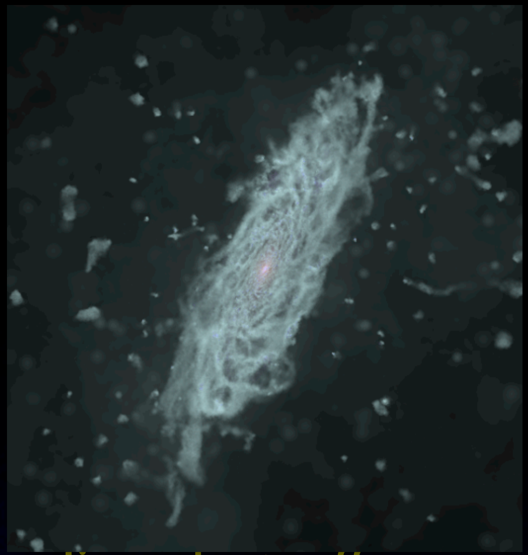

- TreeSPH code Gasoline (Wadsley et al. 2004)
- SF: $d\rho_*/dt = \epsilon_{SF}\rho_{gas}/t_{dyn} \propto \rho_{gas}^{1.5}$ when gas has $n_H > n_{SF}$
- Blastwave feedback model for SN II (Stinson+ 2006): radiative cooling shut-off according to analytical solution from McKee & Ostriker (1977).
- Radiative cooling for H, He and metals were computed using Cloudy (Ferland+ 1998), assuming ionization equilibrium under uniform UVB (Haardt & Madau 2012)
- Turbulent diffusion model (Wadsley+ 2008; Shen+2010) to capture mixing of metals in turbulent outflows.
- Same initial set up as in Eris (Guedes+2011)

Galaxy	m_{DM} (Ms)	m_{SPH} (Ms)	ϵ_G (pc)	n_{SF} (cm^{-3})
Eris2	9.8×10^4	2×10^4	120	20.0

Very high resolution - 4 M particles within Rvir at z =2.8, to resolve the galaxy structure, the progenitor satellites and dwarfs

High SF threshold, allow the inhomogeneous SF site to be resolved and localize feedback

Metal Cooling Under UV Radiation

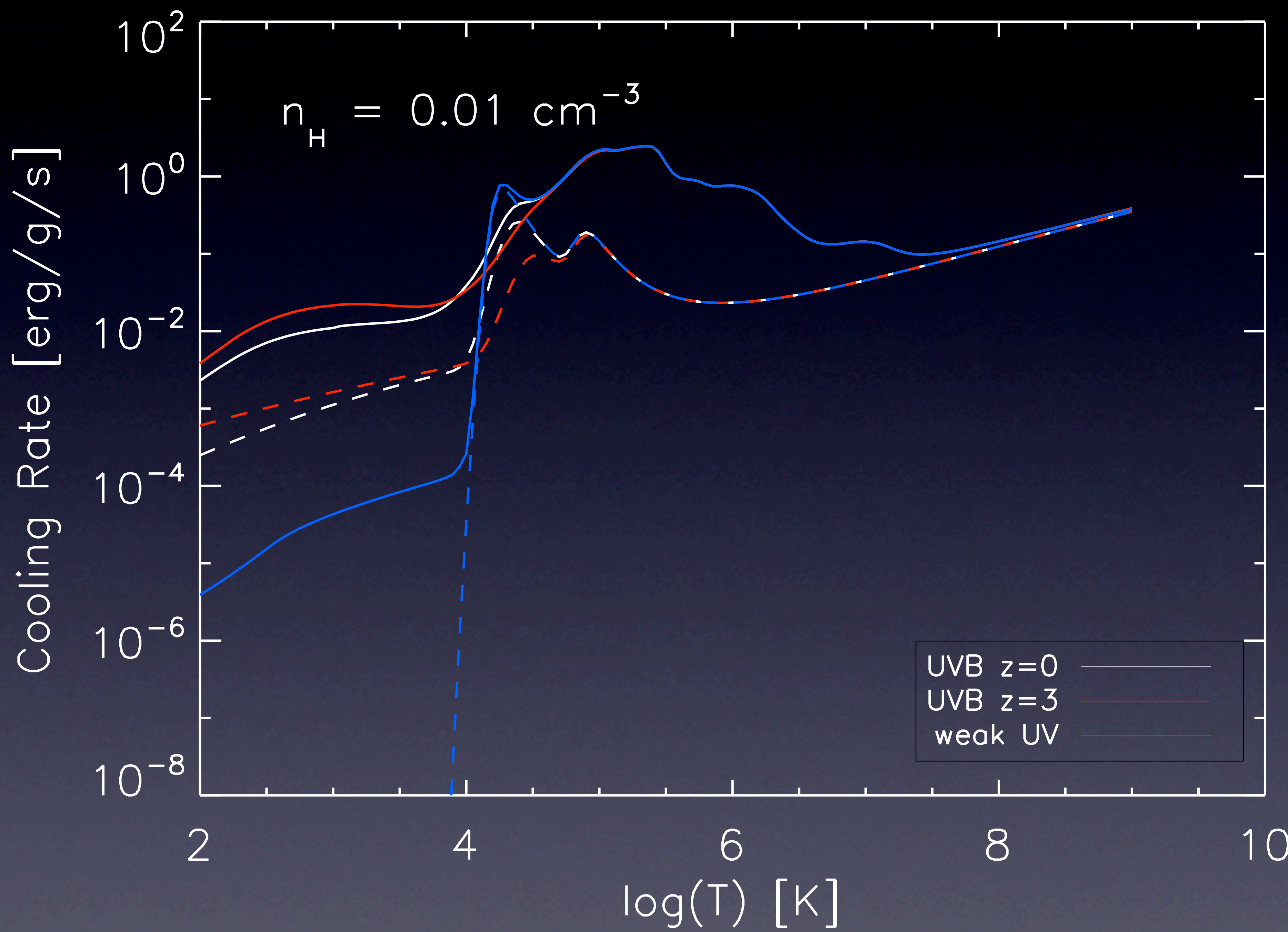

- Metal cooling computed using CLOUDY (Ferland 1998)
- With UVB from Haardt & Madau (2001)
- Function of ρ, T, Z, z

Shen+. 2010

Metal Cooling Under UV Radiation

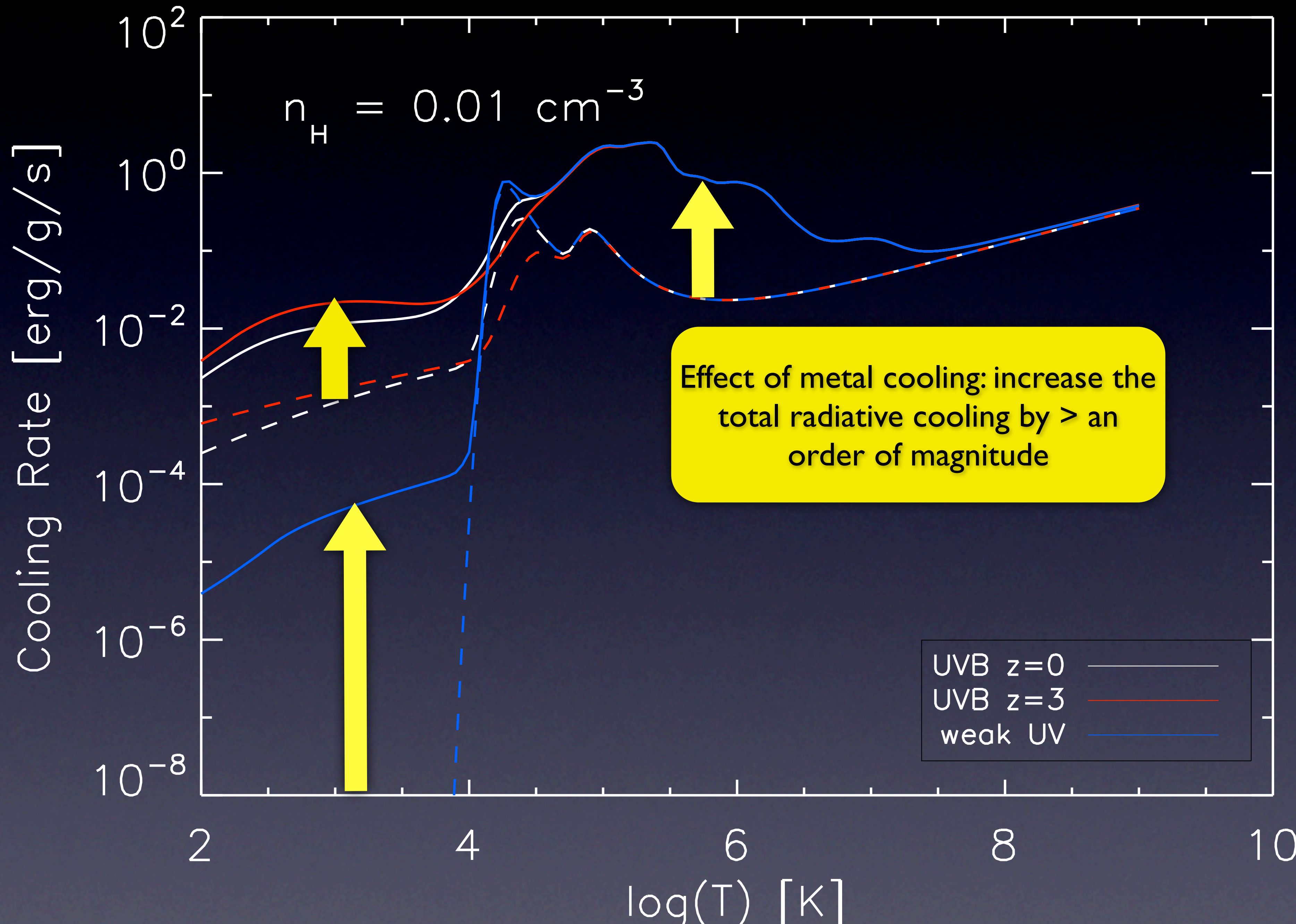

- Metal cooling computed using CLOUDY (Ferland 1998)
- With UVB from Haardt & Madau (2001)
- Function of ρ, T, Z, z

Shen+. 2010

Metal Cooling Under UV Radiation

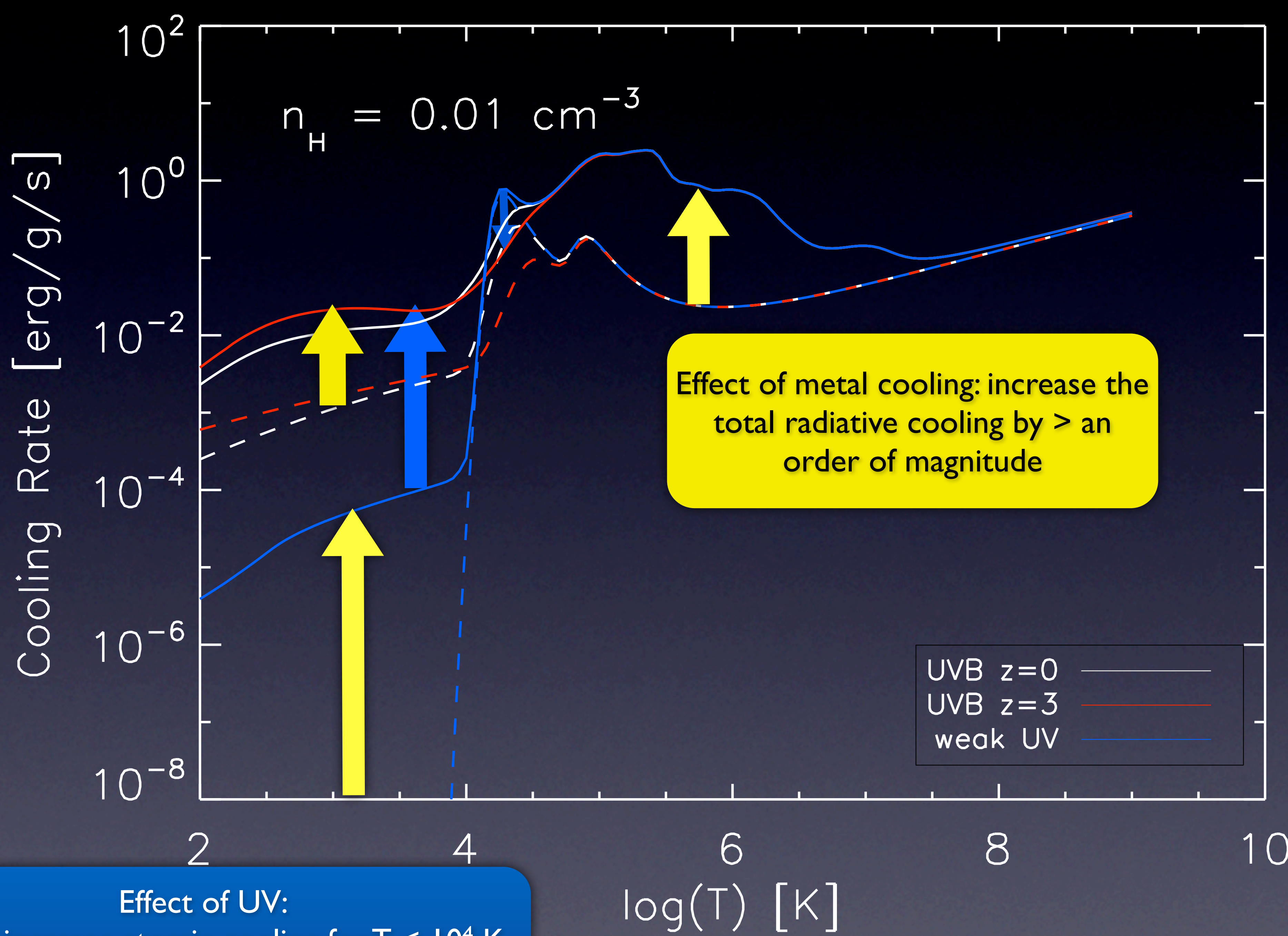

Effect of UV:
Largely increase atomic cooling for T < 10^4 K
Decease the cooling at T > 10^4 K (more significant for lower density gas)

- Metal cooling computed using CLOUDY (Ferland 1998)
- With UVB from Haardt & Madau (2001)
- Function of ρ, T, Z, z

Shen+. 2010

Smagorinsky Model of Turbulent Diffusion

Wadsley+ (2008); Shen+(2010)

- Most basic turbulent model: (κ_{Turb} has units of velocity × length)

$$\frac{\partial \bar{u}}{\partial t} + \bar{\mathrm{v}}.\nabla\bar{u} = -(\gamma - 1)\bar{u}(\nabla.\bar{\mathrm{v}}) + \nabla\kappa_{\mathrm{Turb}}\nabla\bar{u}$$

- Smagorinsky model (Mon. Weather Review 1963) -- Diffusion Coefficient determined by velocity Shear

$$\kappa_{Turb} = l_S{}^2 S, \ \ S = \sqrt{S_{ij}S_{ij}}$$

- S_{ij} = trace-free strain rate of resolved flow; l_s = Smagorinsky length. For incompressible grid models $l_s^2 \sim 0.02\ \Delta x^2$

- For SPH we use $\kappa_{Turb} = C\ |S_{ij}|h^2$ with $C \sim 0.05$ (Wadsley, Veeravalli & Couchman 2008; See also Scannapieco & Brüggen 2008, Grief et al 2009)

- After implementation of turbulent diffusion, SPH is able to produce the entropy profile similar to grid codes

Eris2 and Its Metal-Enriched CGM at z = 2.8

Shen+ (2012) arXiV:1205.0270

$M_{vir}(M_{sun})$	R_{vir} (kpc)	$M^*(M_{sun})$	SFR(M_s/yr)	12+log(O/H)	$T>10^5$ K (%)	R_z	$<Z_g>_{vir}$
2.6×10^{11}	50	1.5×10^{10}	20	8.50	54%	~5 Rvir	0.7 Z_{sun}

- At z=2.8, Eris2 has M_{vir} and M_* close to an LBG but lower than typical observed LBGs (e.g, Steidel+ 2010)
- More than half of metals locked in the warm-hot ($T > 10^5$) phase
- Cold, SF gas has 12+log(O/H)=8.5, within the M_*-Z relationship (Erb +2006)
- The metal "bubble" extends up to 250 kpc, 5 R_{vir}

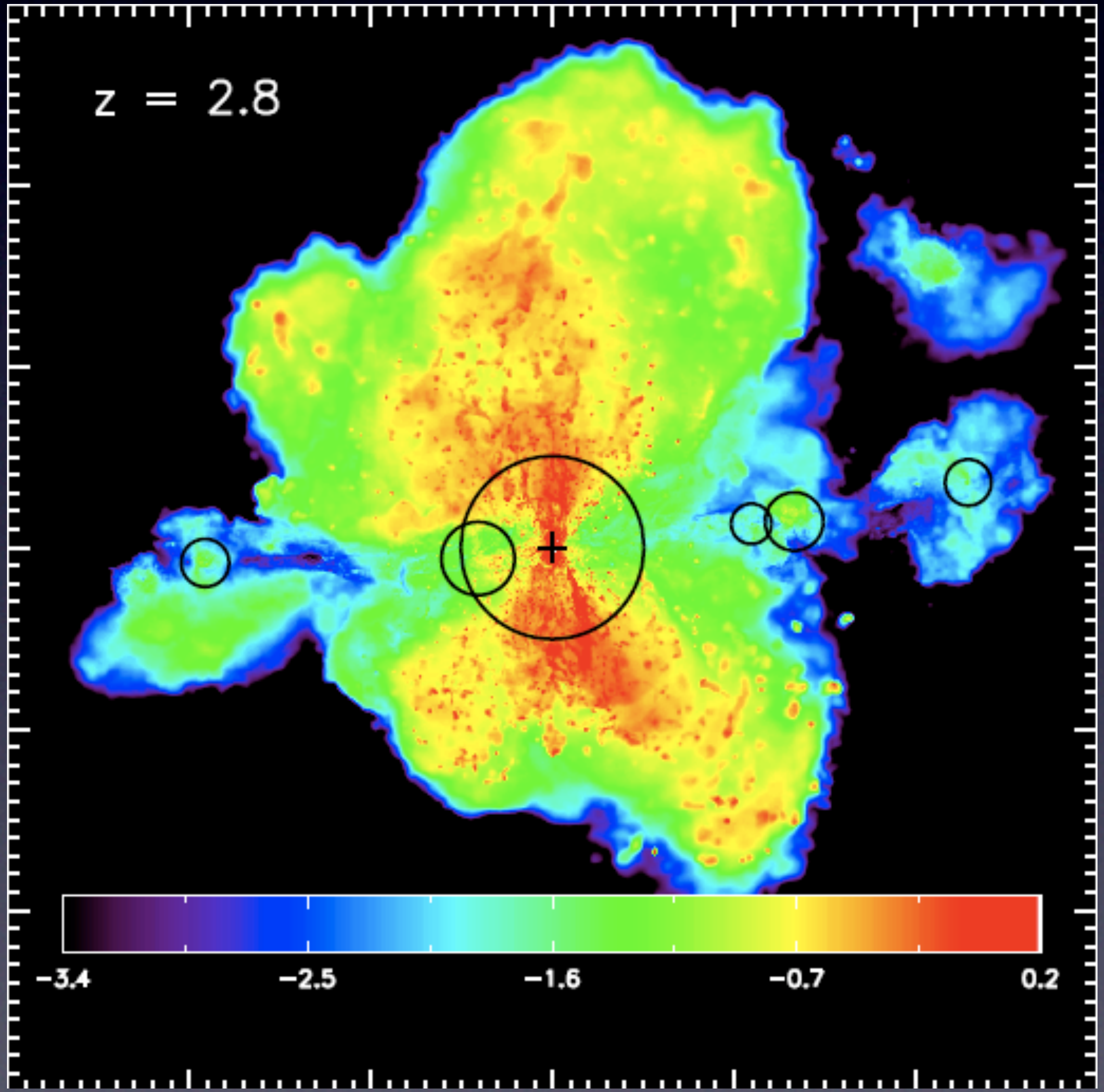

600 x 600 x 600 kpc3 projected map of gas metallicity. The disk is viewed nearly edge on

Kinematics of the Metal-Enriched CGM

- 600 x 600 x 10 kpc slice, projected to x-y plane, disk nearly edge-on
- Max projected averaged velocity ~300 km/s (host)
- Metallicity is high along the miner axis but non-zero along the major axis (Rubin + 2012; Kacprzak+2012)
- Average outflow velocity decrease at larger distances and join the inflow -- halo fountain (Oppenheimer+ 2010)

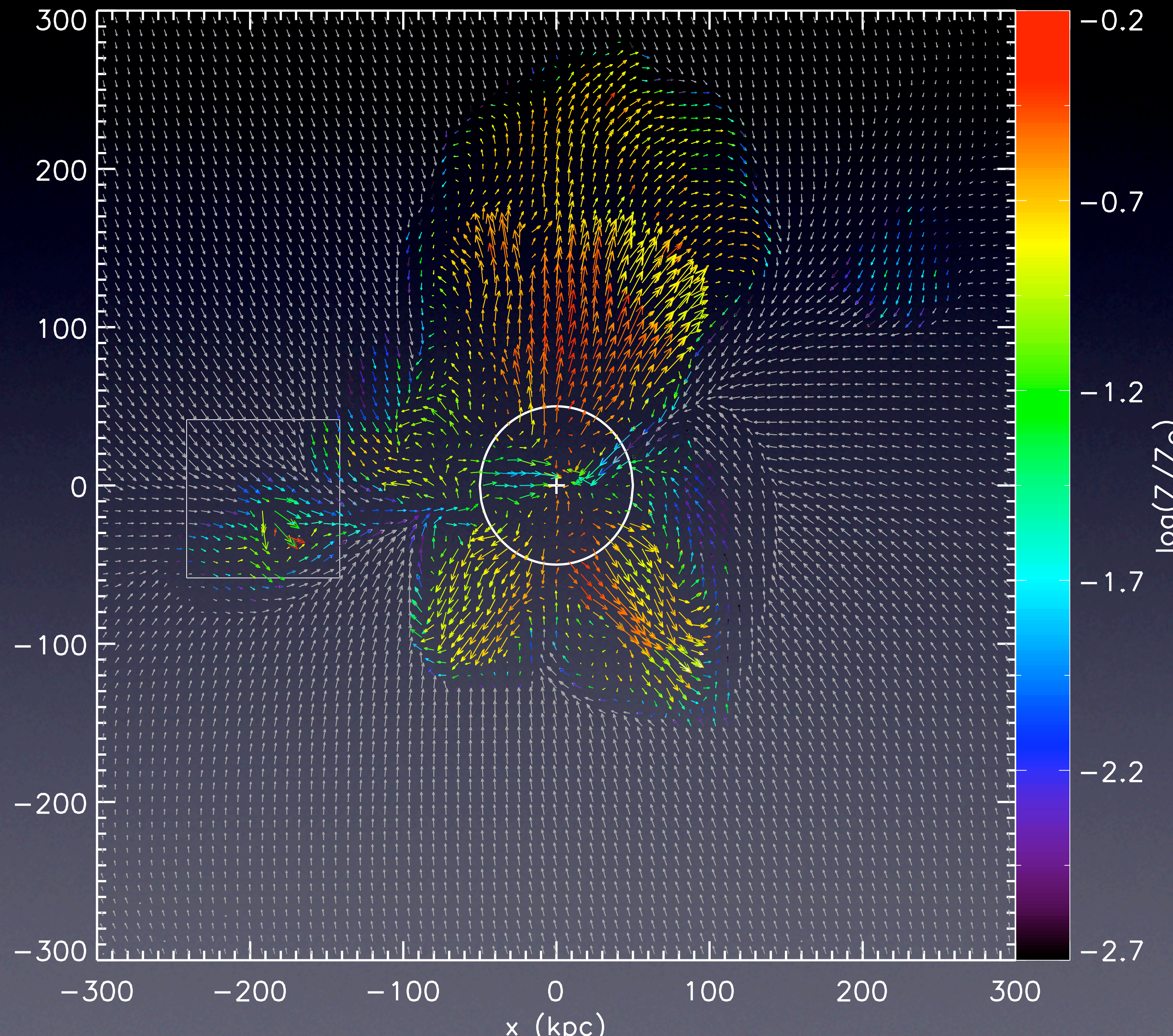

Kinematics of the Metal-Enriched CGM

- 600 x 600 x 10 kpc slice, projected to x-y plane, disk nearly edge-on
- Max projected averaged velocity ~300 km/s (host)
- Metallicity is high along the miner axis but non-zero along the major axis (Rubin + 2012; Kacprzak+2012)
- Average outflow velocity decrease at larger distances and join the inflow -- halo fountain (Oppenheimer+ 2010)

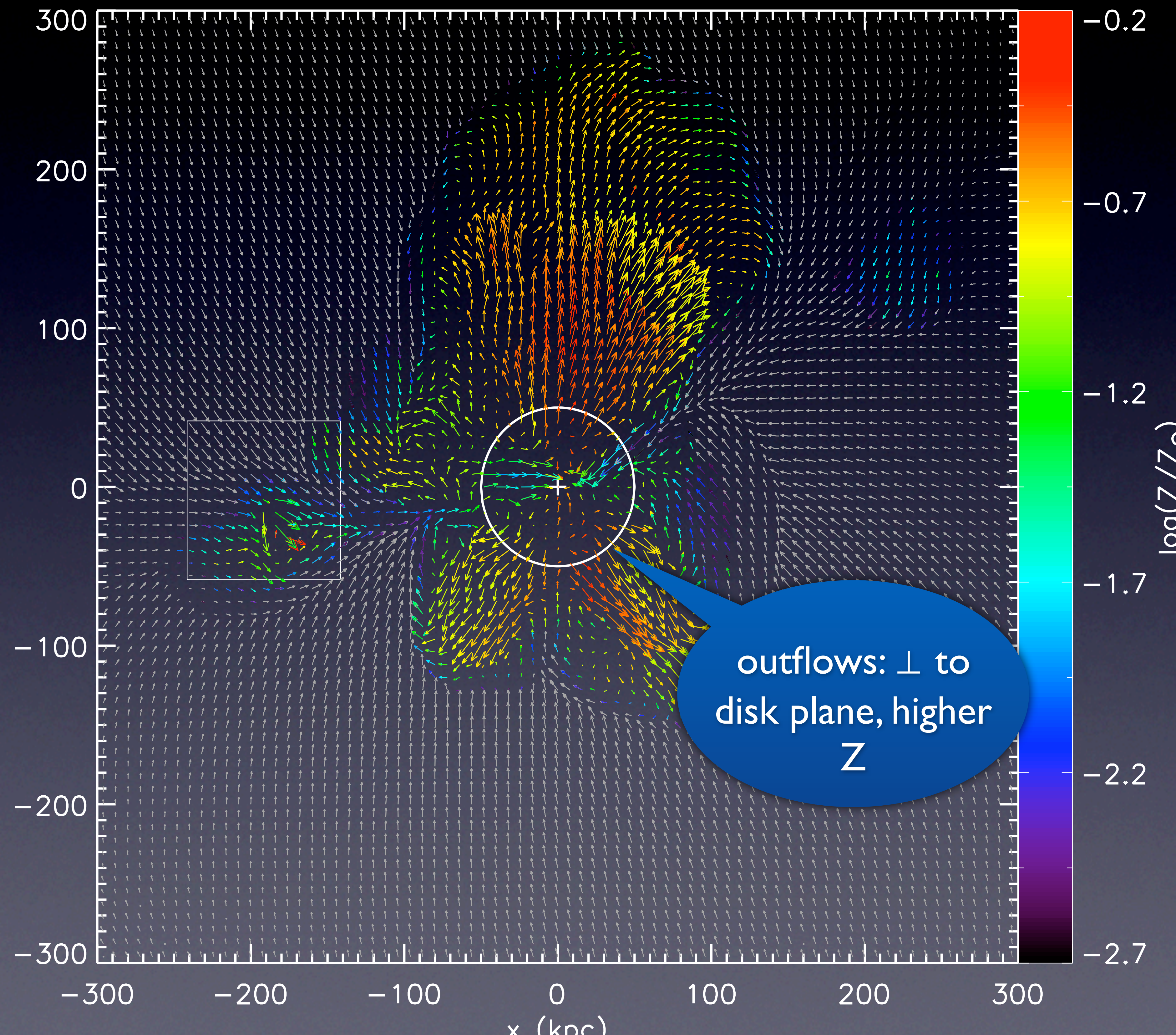

Kinematics of the Metal-Enriched CGM

- 600 x 600 x 10 kpc slice, projected to x-y plane, disk nearly edge-on
- Max projected averaged velocity ~300 km/s (host)
- Metallicity is high along the miner axis but non-zero along the major axis (Rubin + 2012; Kacprzak+2012)
- Average outflow velocity decrease at larger distances and join the inflow -- halo fountain (Oppenheimer+ 2010)

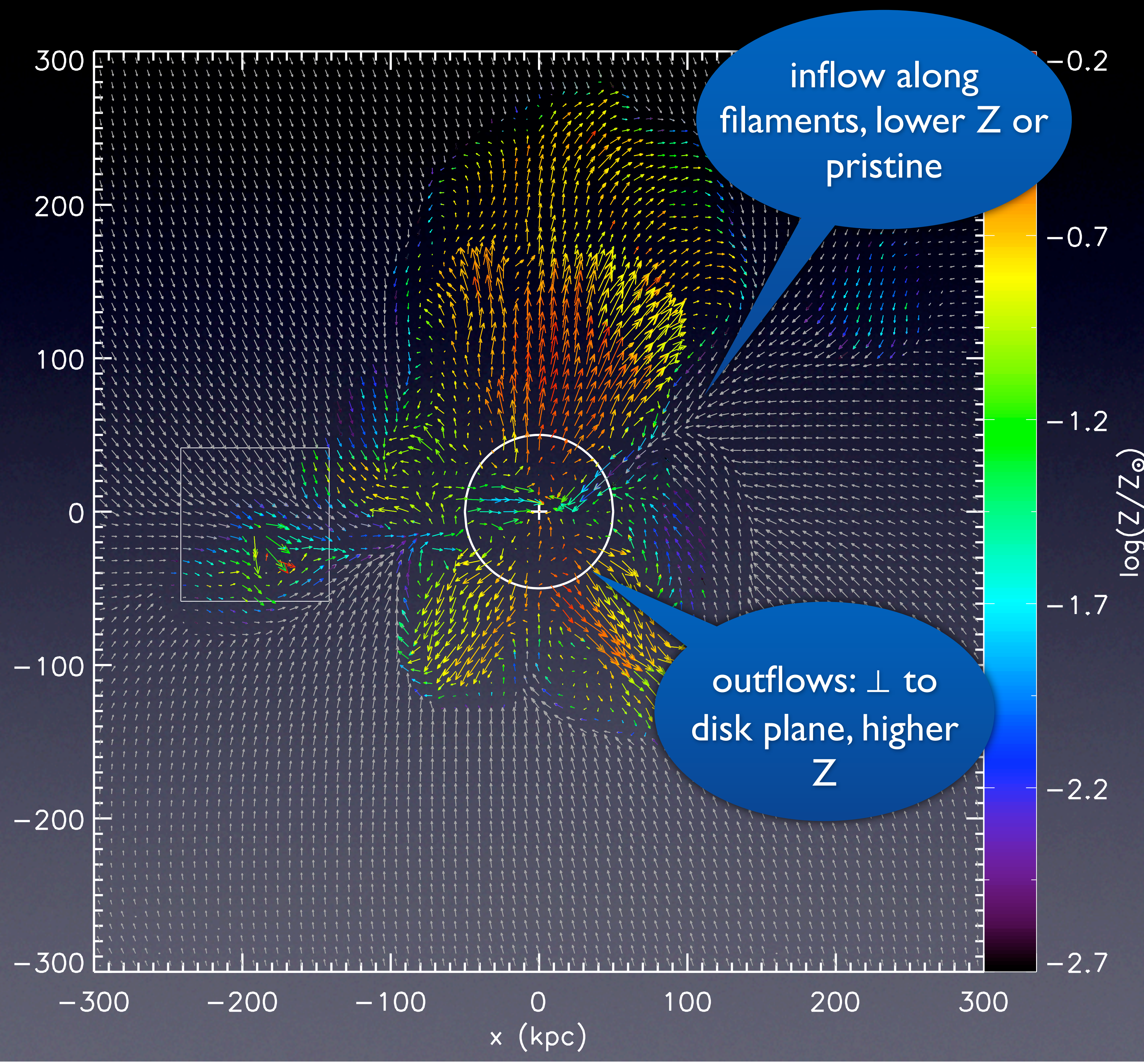

Kinematics of the Metal-Enriched CGM

- 600 x 600 x 10 kpc slice, projected to x-y plane, disk nearly edge-on
- Max projected averaged velocity ~300 km/s (host)
- Metallicity is high along the miner axis but non-zero along the major axis (Rubin + 2012; Kacprzak+2012)
- Average outflow velocity decrease at larger distances and join the inflow -- halo fountain (Oppenheimer+ 2010)

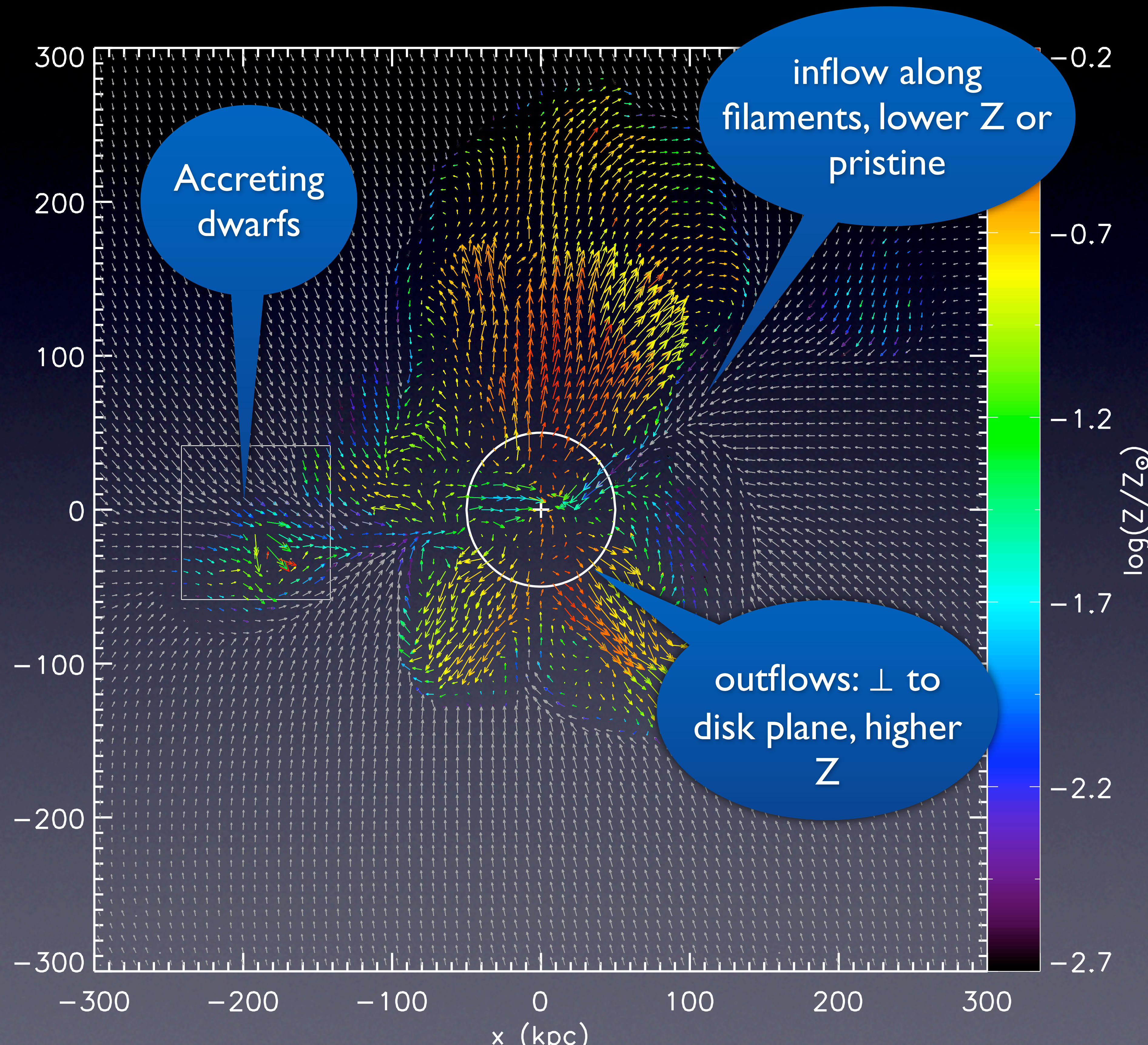

Computing Fraction of Ions & Column Density Map

- Post-processing using photo-ionization code Cloudy (Ferland+ 1998)
- Incident radiation includes the extragalactic UV background (Haardt & Madau 2012) and stellar UV
- Stellar UV radiation: using Starburst99 (Leitherer+ 1999), assuming a constant SFR of 20 M_{sun}/yr.
- Escape fraction f_{esc} = 3%, $J_d = J_0/(4\pi d^2)$
- Assuming gas is *optically thin:* not valid for column N_{HI} above LLS.

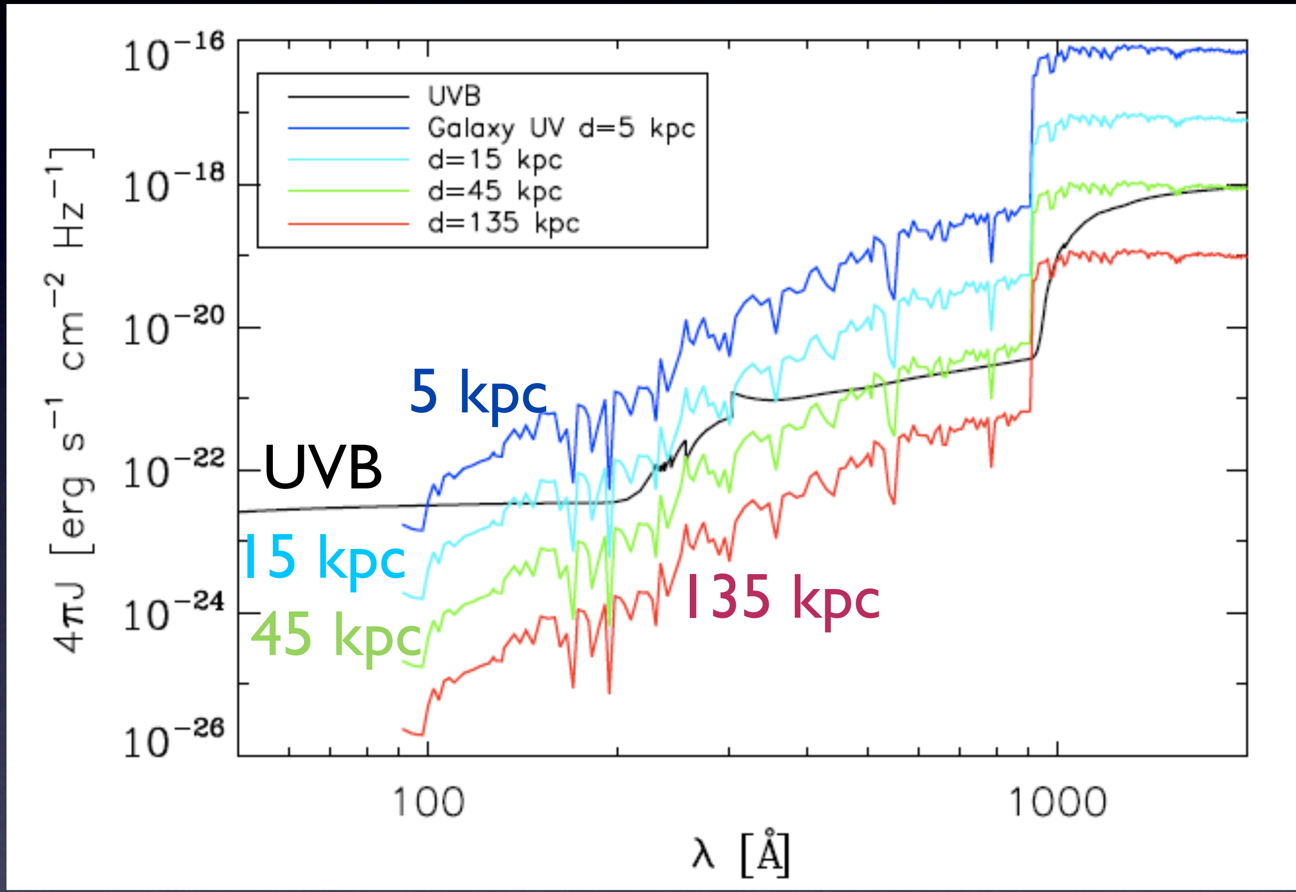

Photo-ionization heating due to local UV radiation is *not* taken into account.

Computing Fraction of Ions & Column Density Map

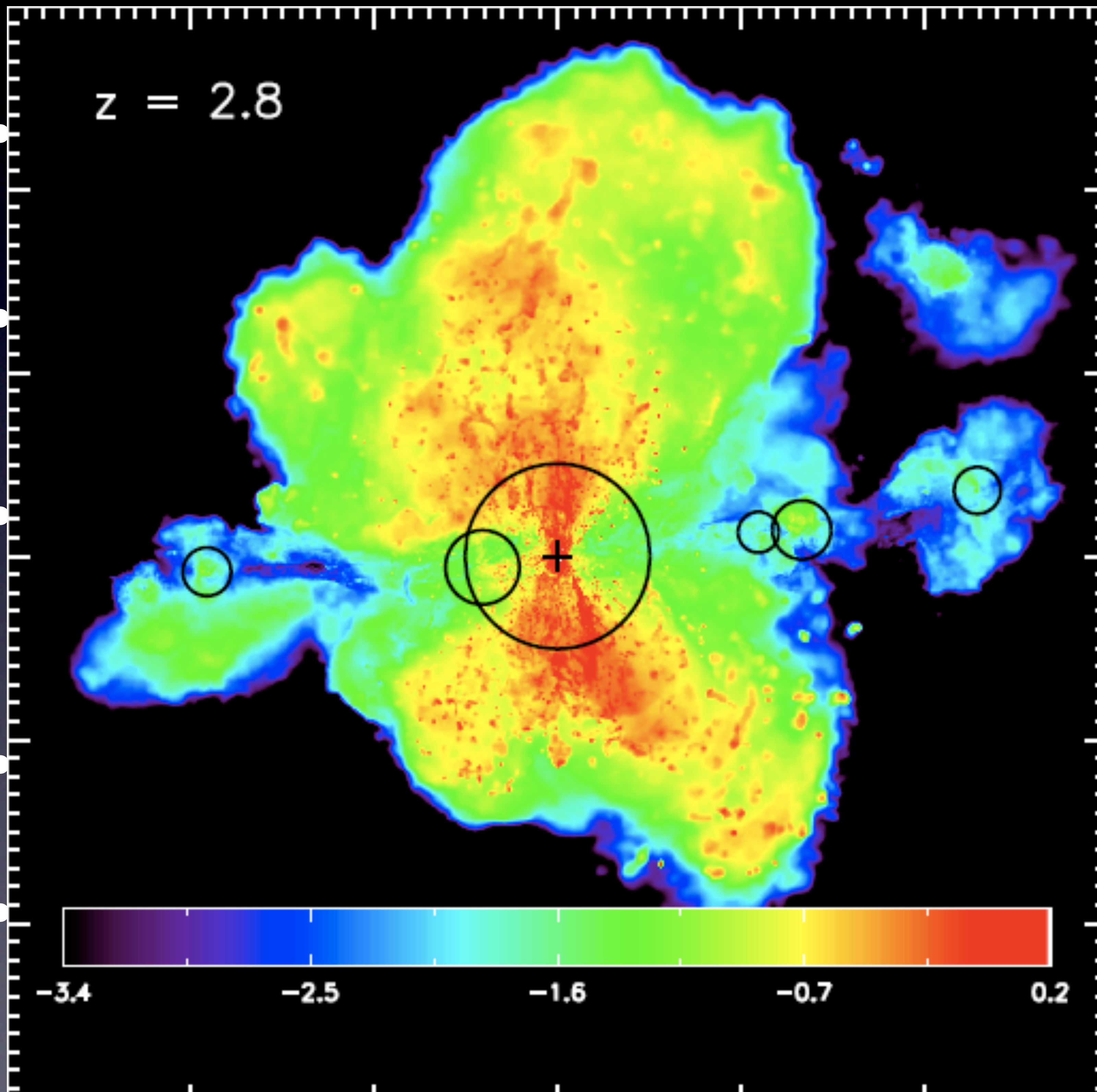

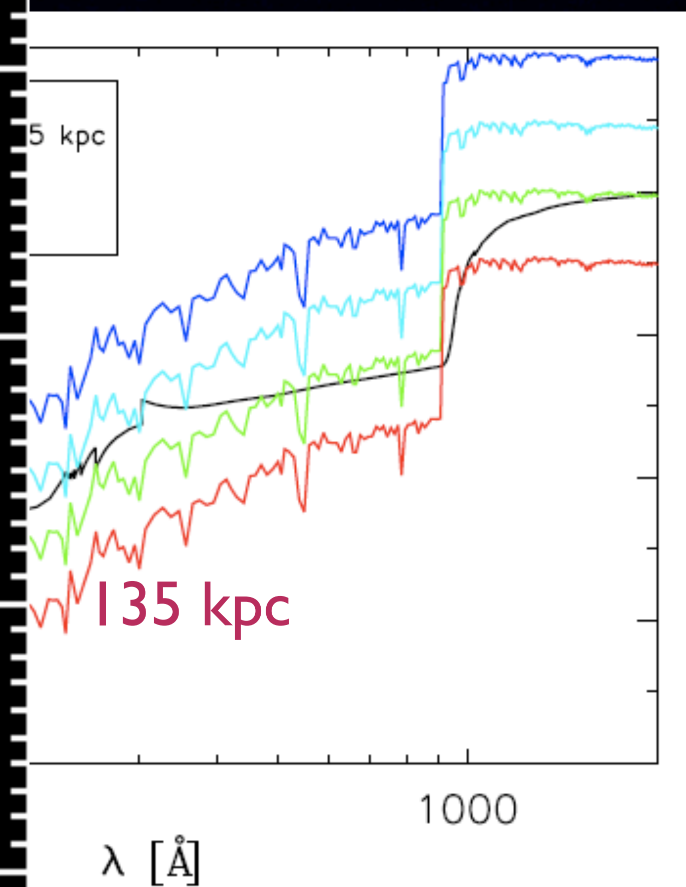

eating due to local UV
taken into account.

Computing Fraction of Ions & Column Density Map

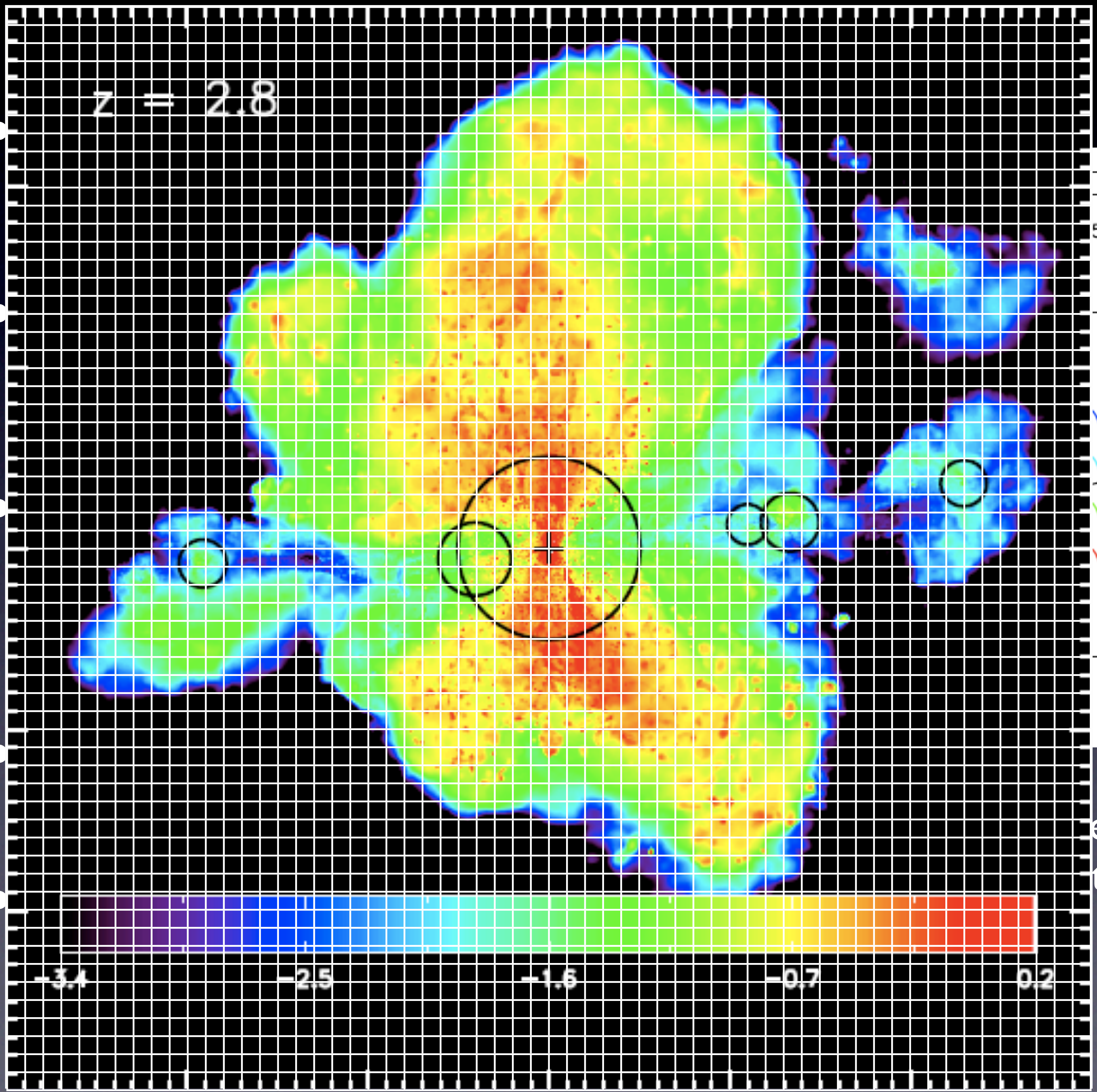

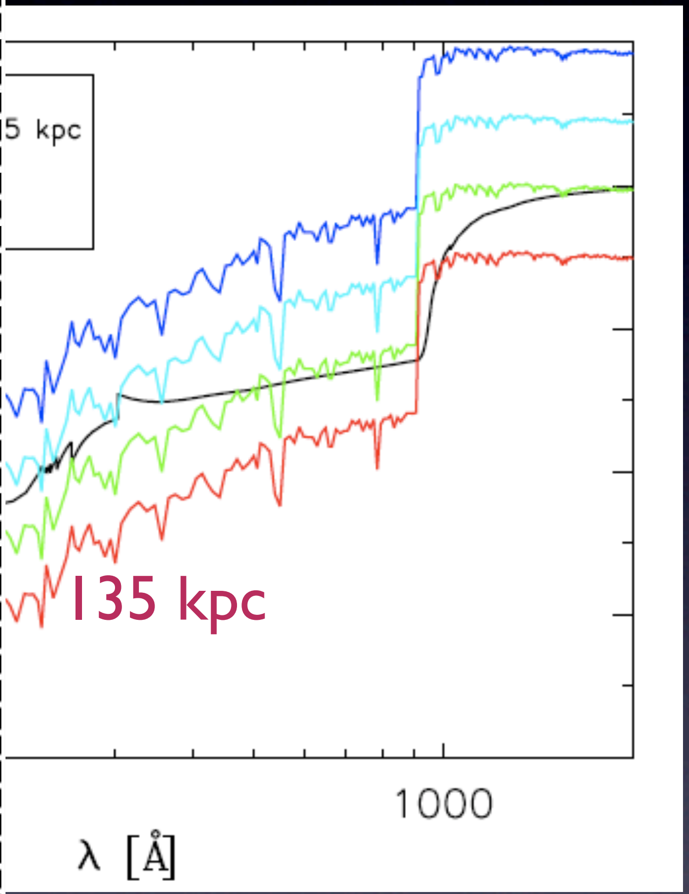

eating due to local UV
taken into account.

CGM Metals Traced by Different Ions

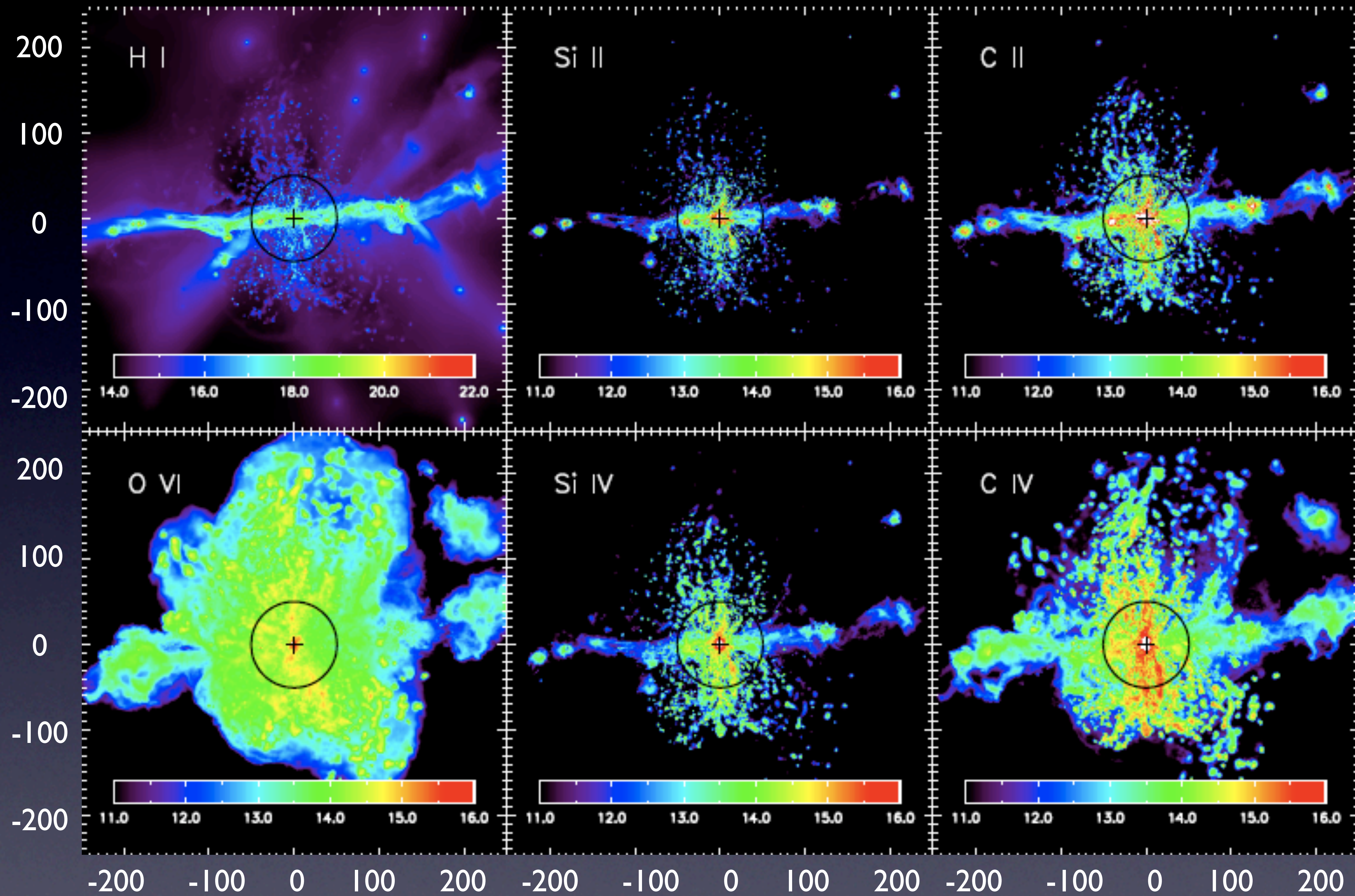

HI: 10^{14}-10^{21} cm^{-2}

Metals: 10^{11}-10^{16} cm^{-2}

Calculating ion fractions:

- UVB + non-uniform stellar UV assuming constant SFR 20 Msun/yr
- Photo-heating of local UV not included
- Assuming optically thin

- Multi-phase CGM: low and high ions co-exist in same absorbers
- Covering factors of low ions (C II, Si II) decrease more rapidly than high ions
- O VI has large covering factor up to 4 $R_{vir,}$ M_O(CGM) ~5x 10^7 M_{sun}> M_O(ISM)

High ions: Collisional Ionization or Photoionization?

Cooler (T~3-5 $\times 10^4$ K), clumpier, photoionized OVI

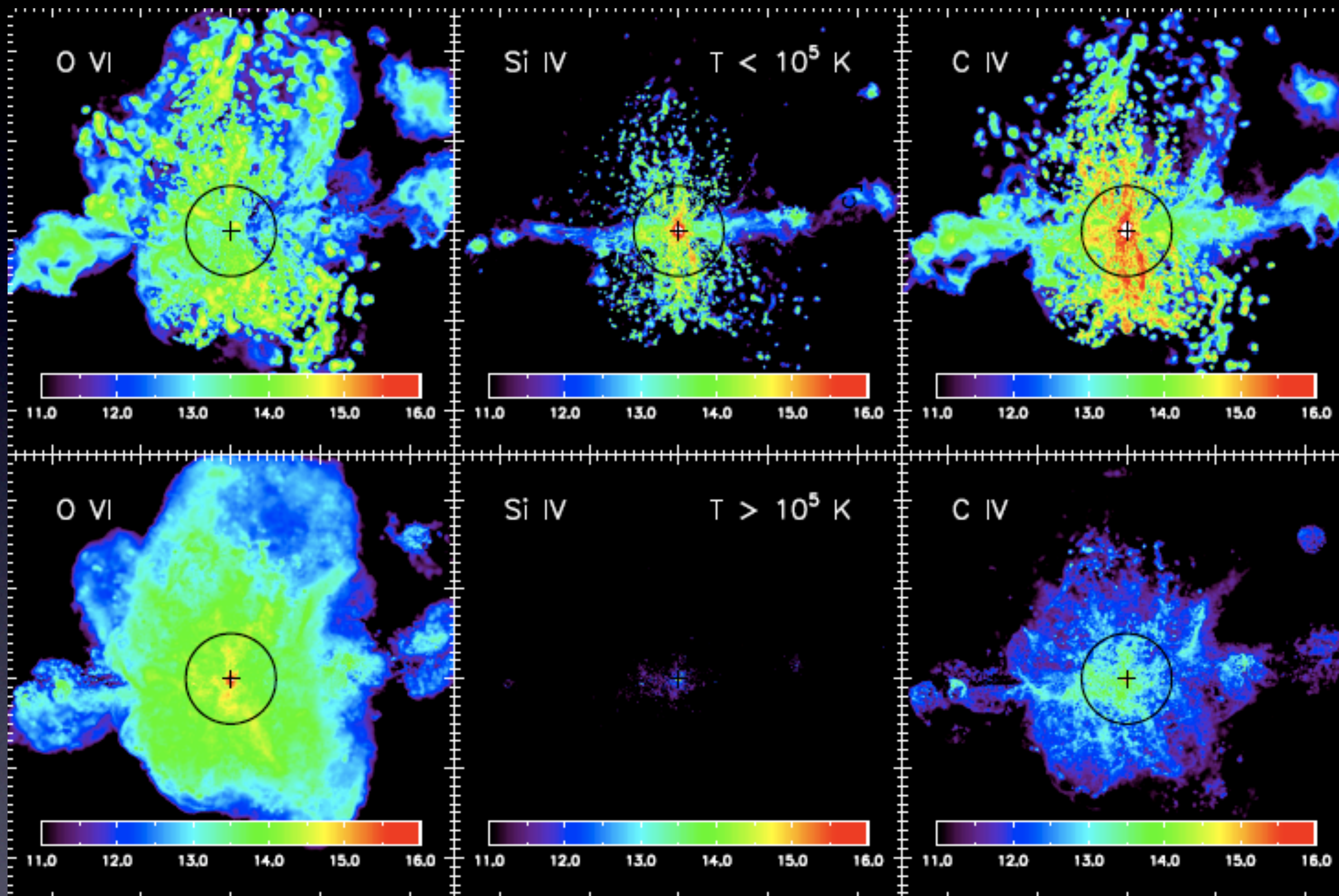

Si IV and C IV: Mostly photo-ionized

Hotter (T>10^5K), more diffuse, collisionally ionized OVI

- O VI: mostly collisional ionized within 2 Rvir, but photo-ionized at larger distance

Inflowing and Outflowing CGM

- Coexistence of inflow and outflow in the CGM:

- H I: cold inflow perpetrates viral radius. with $2R_{vir}$, 90% system with $N_{HI} > 10^{17.2}$ cm^{s} (LLS) is inflowing.
- Outflow gas increases the H I covering factor at large b.
- Low ions (C II or Si II) similar to H I

  - O VI: by mass 68% outflow, 32% inflow
  - C IV & Si IV: inflow and outflow contribute similarly

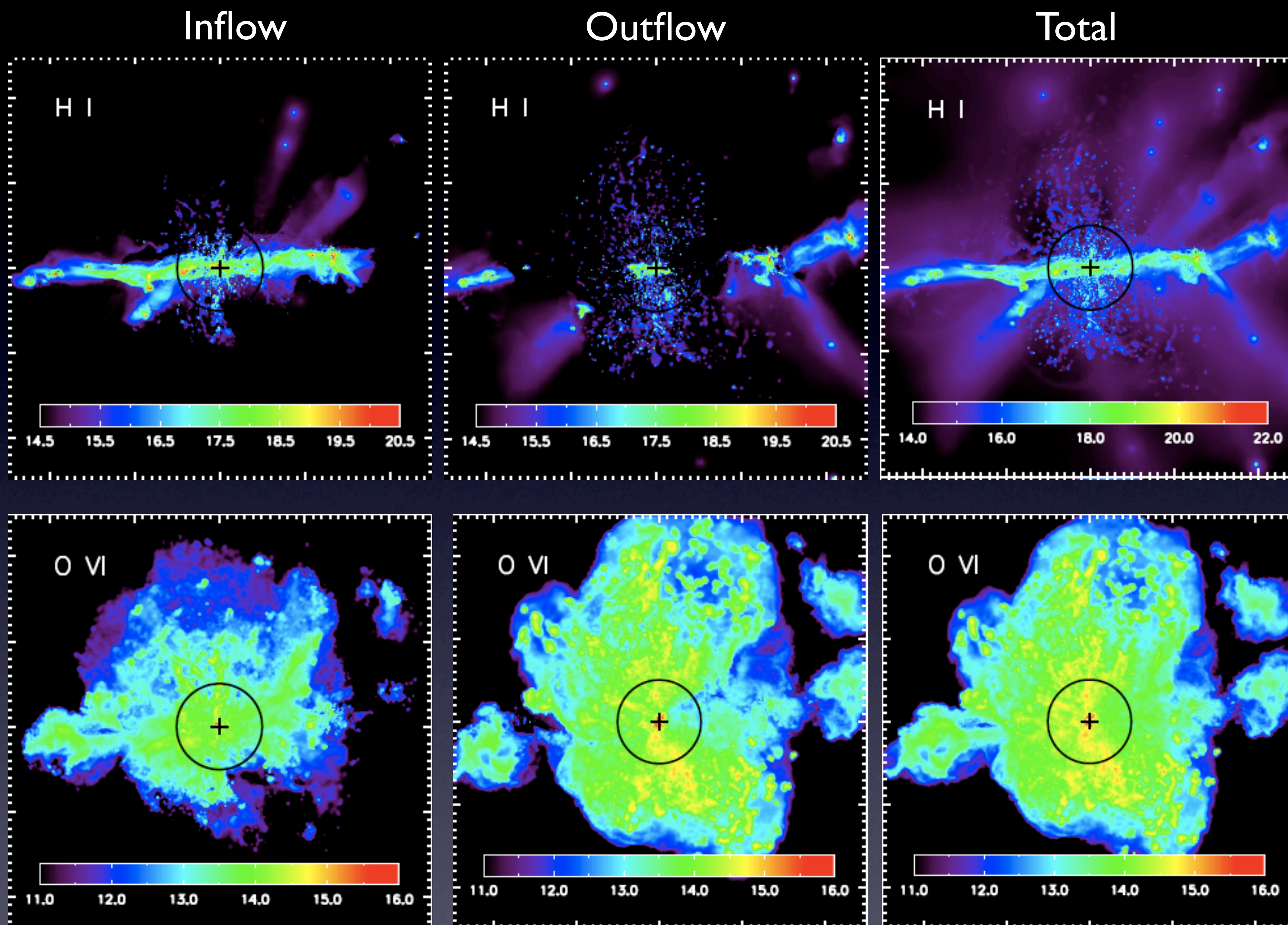

	H I	Si II	C II	Si IV	C IV	O VI
Inflow mass (%)	77%	66%	66%	50%	44%	32%

Synthetic Absorption Spectra

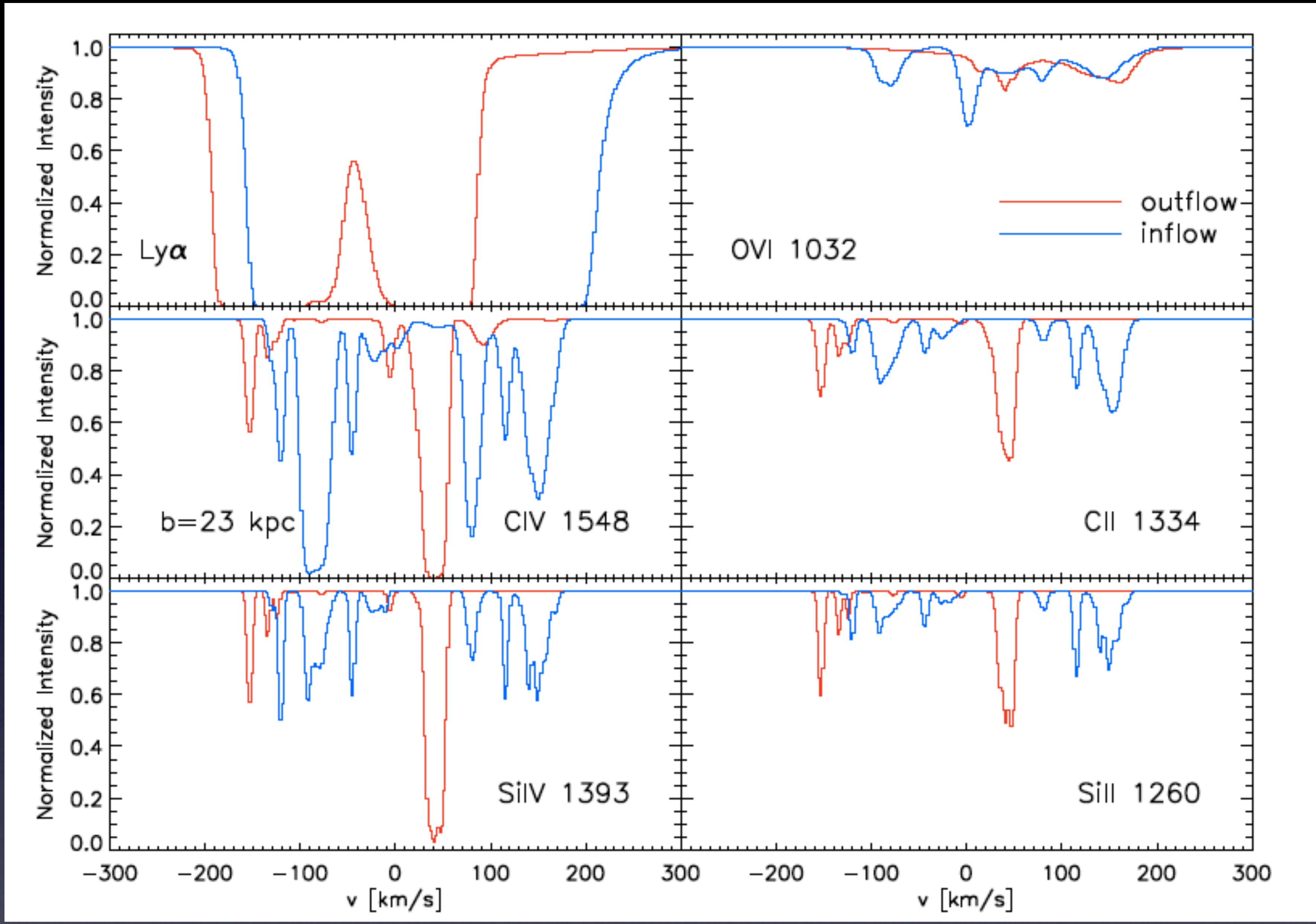

- Optical depth $\tau(\nu) = \sum_j (m_j Z_j / m) W_{2D}(r_{jl}, h_j) \sigma_j(\nu)$; $\sigma_j(\nu)$ - cross section (Voigt function), $W_{2D}(r_{jl}, h_j)$ - 2D SPH kernel
- Rest frame equivalent width: $W_0 = c/\nu_0^2 \int [1 - e^{-\tau(\nu)}] d\nu$

Synthetic Absorption Spectra

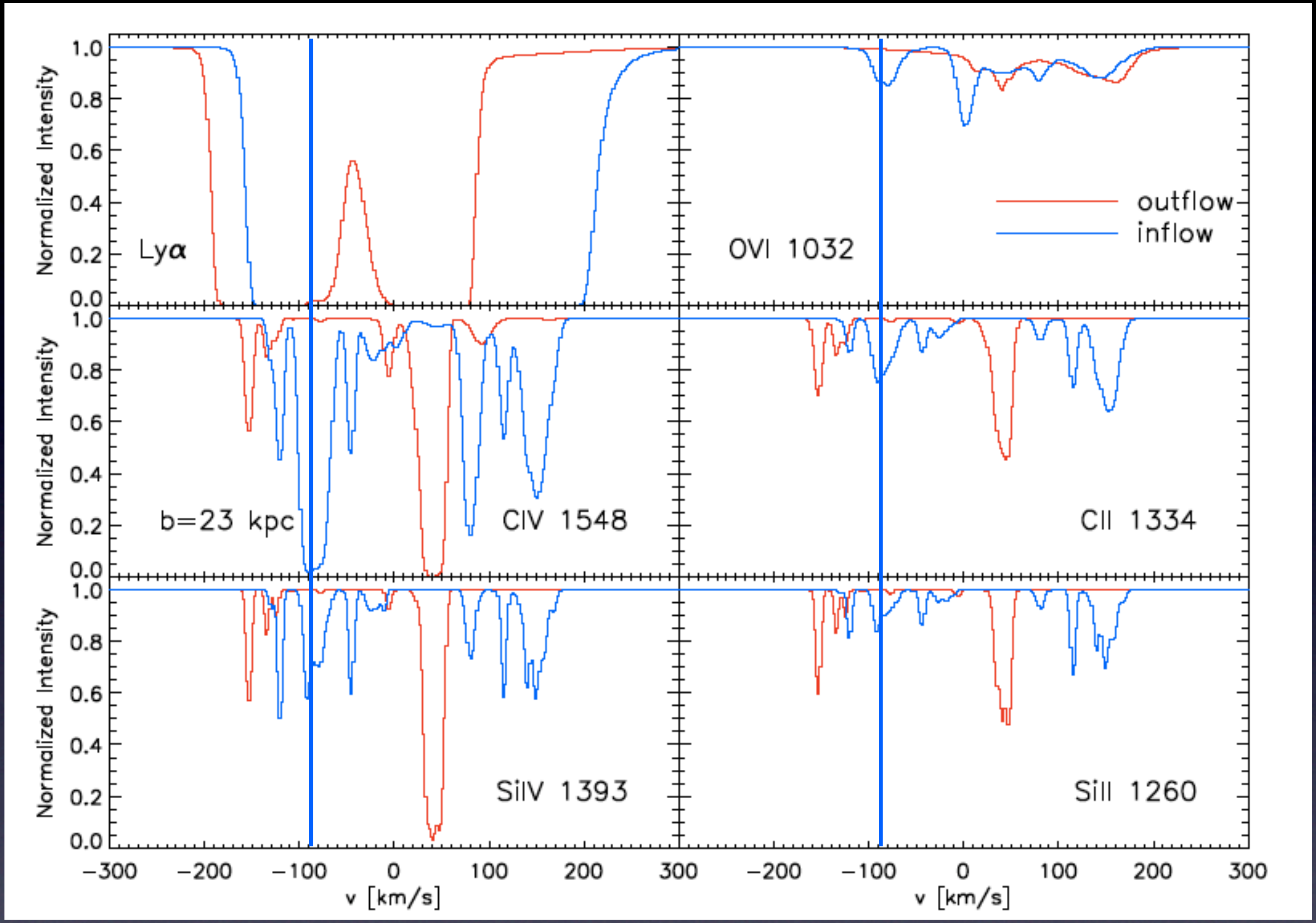

- Optical depth $\tau(\nu) = \sum_j (m_j Z_j/m) W_{2D}(r_{jl}, h_j)\sigma_j(\nu)$; $\sigma_j(\nu)$ - cross section (Voigt function), $W_{2D}(r_{jl}, h_j)$ - 2D SPH kernel
- Rest frame equivalent width: $W_0 = c/\nu_0^2 \int [1-e^{-\tau(\nu)}]d\nu$

Synthetic Absorption Spectra

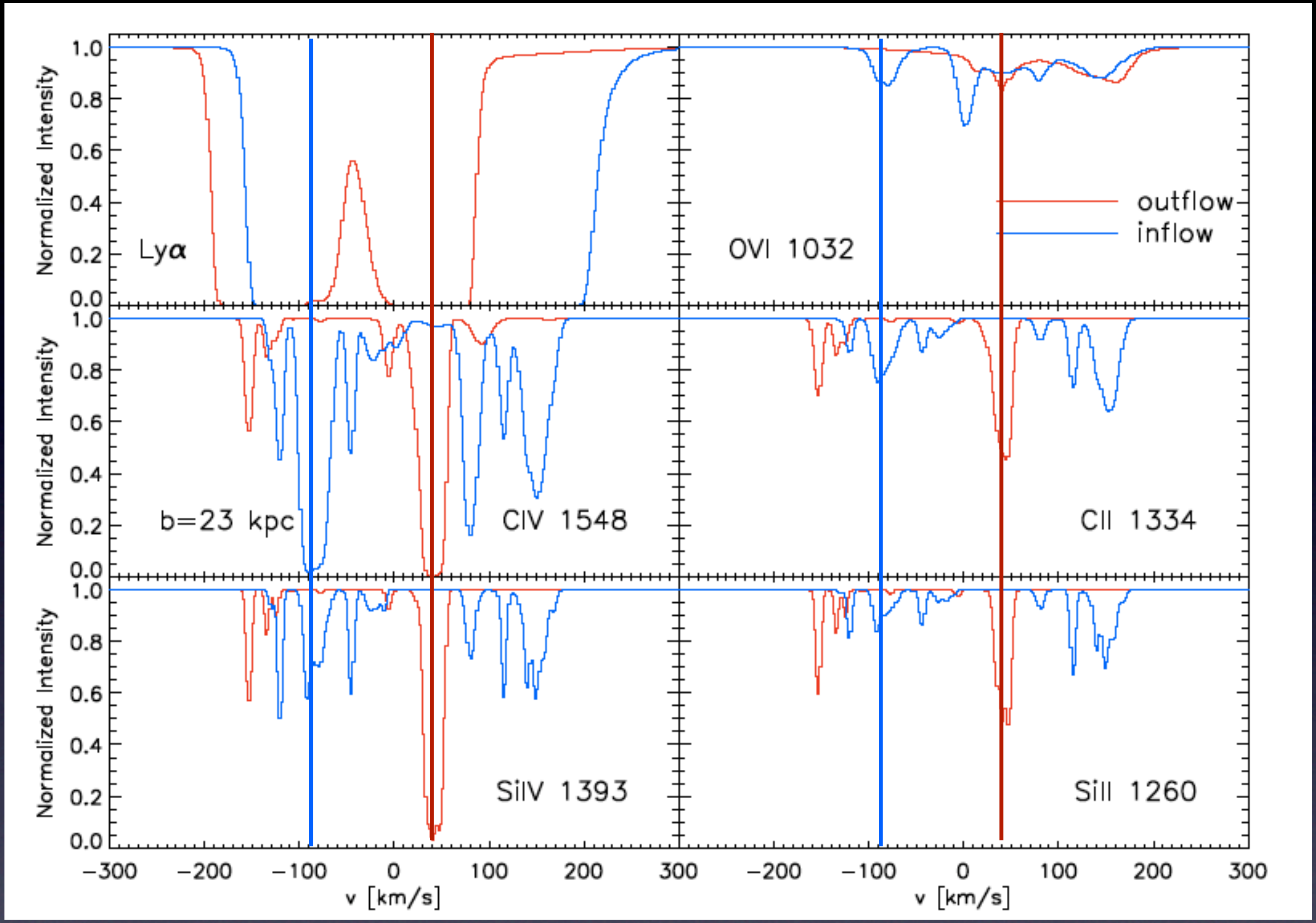

- Optical depth $\tau(\nu) = \sum_j (m_j Z_j/m) W_{2D}(r_{jl}, h_j)\sigma_j(\nu)$; $\sigma_j(\nu)$ - cross section (Voigt function), $W_{2D}(r_{jl}, h_j)$ - 2D SPH kernel

- Rest frame equivalent width: $W_0 = c/\nu_0^2 \int [1-e^{-\tau(\nu)}]d\nu$

Synthetic Absorption Spectra

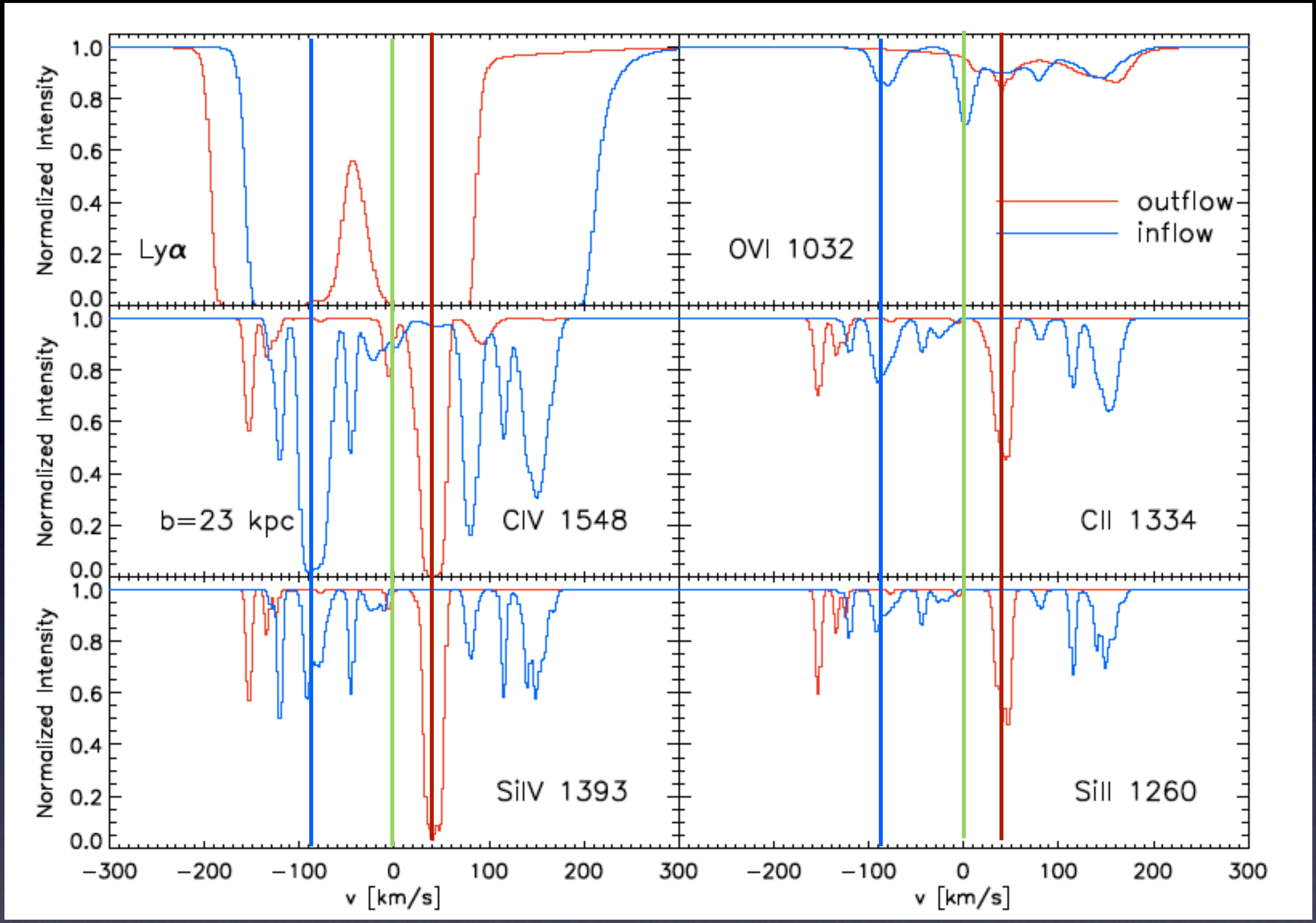

- Most, but not all, components exist in both high and low ions -- Multi-phase nature of absorbers

- Optical depth $\tau(\nu) = \sum_j (m_j Z_j/m) W_{2D}(r_{jl}, h_j)\sigma_j(\nu)$; $\sigma_j(\nu)$ - cross section (Voigt function), $W_{2D}(r_{jl}, h_j)$ - 2D SPH kernel
- Rest frame equivalent width: $W_0 = c/\nu_0^2 \int [1-e^{-\tau(\nu)}]d\nu$

Synthetic Absorption Spectra

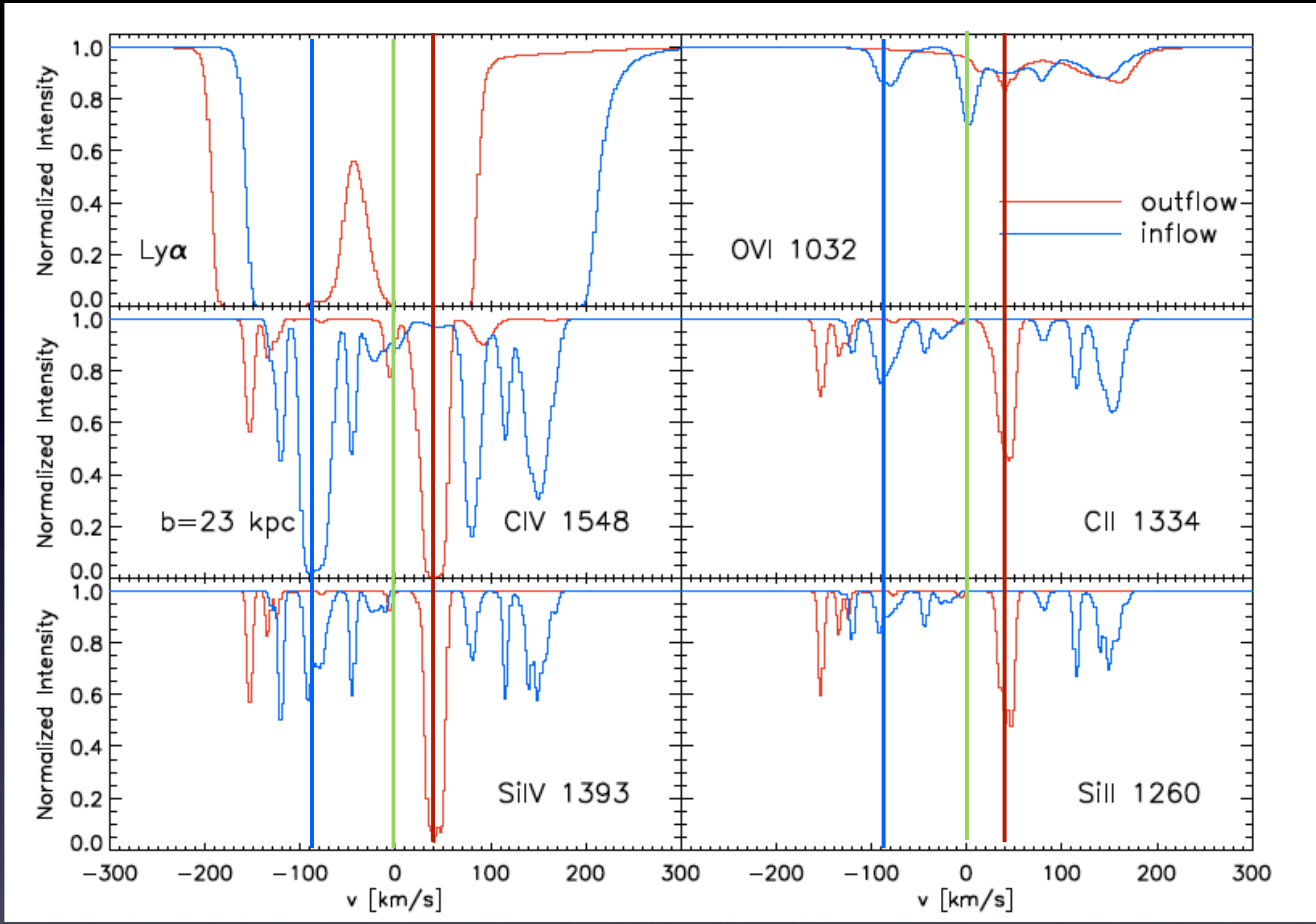

- Most, but not all, components exist in both high and low ions -- Multi-phase nature of absorbers
- Velocity range ~ ± 300 km/s

- Optical depth $\tau(\nu) = \sum_j (m_j Z_j/m) W_{2D}(r_{jl}, h_j)\sigma_j(\nu)$; $\sigma_j(\nu)$ - cross section (Voigt function), $W_{2D}(r_{jl}, h_j)$ - 2D SPH kernel

- Rest frame equivalent width: $W_0 = c/\nu_0^2 \int [1-e^{-\tau(\nu)}]d\nu$

Synthetic Absorption Spectra

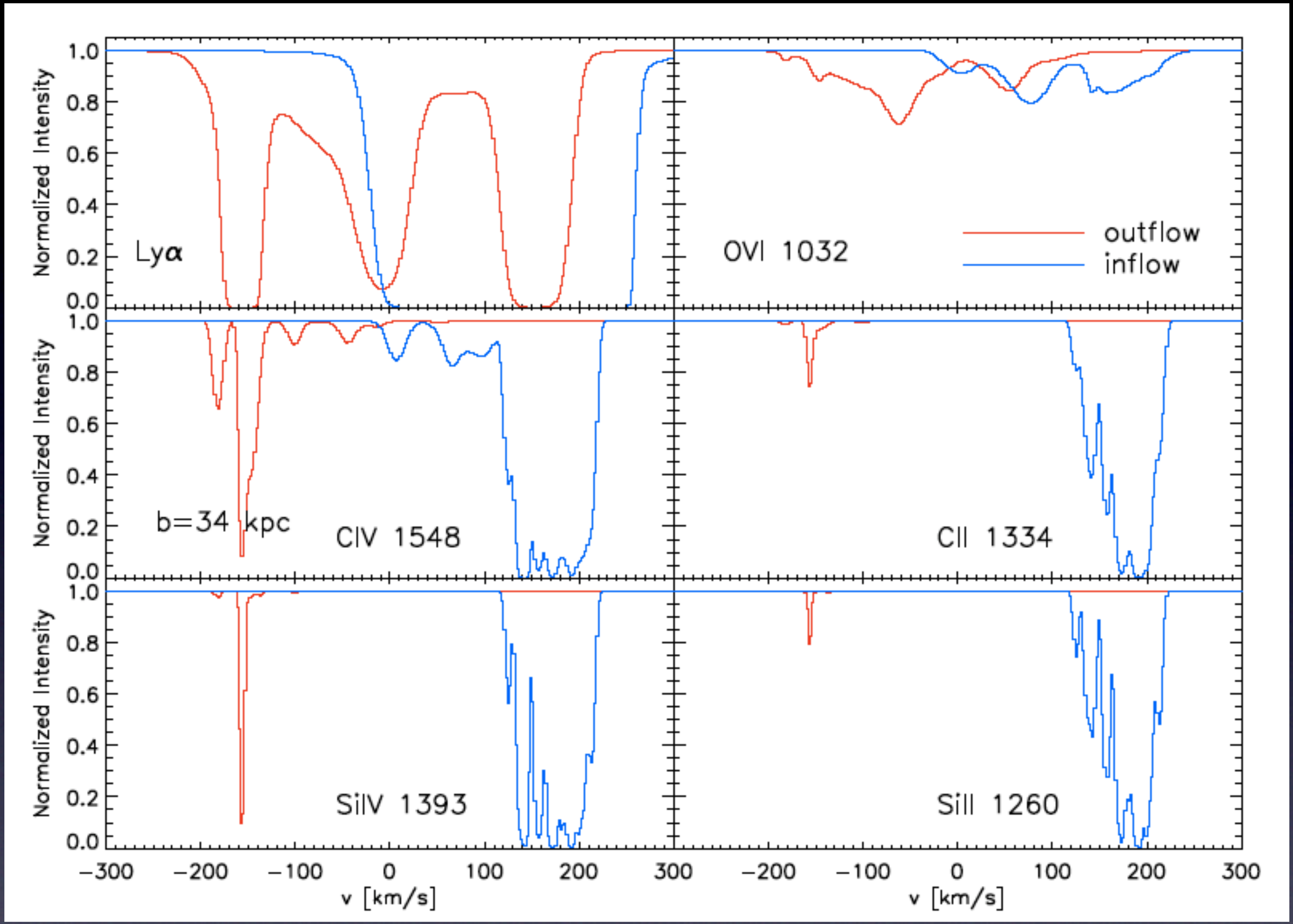

- Most, but not all, components exist in both high and low ions -- Multi-phase nature of absorbers
- Velocity range ~ ± 300 km/s

- Optical depth $\tau(\nu) = \sum_j (m_j Z_j/m) W_{2D}(r_{jl}, h_j)\sigma_j(\nu)$; $\sigma_j(\nu)$ - cross section (Voigt function), $W_{2D}(r_{jl}, h_j)$ - 2D SPH kernel
- Rest frame equivalent width: $W_0 = c/\nu_0^2 \int [1-e^{-\tau(\nu)}]d\nu$

Synthetic Absorption Spectra

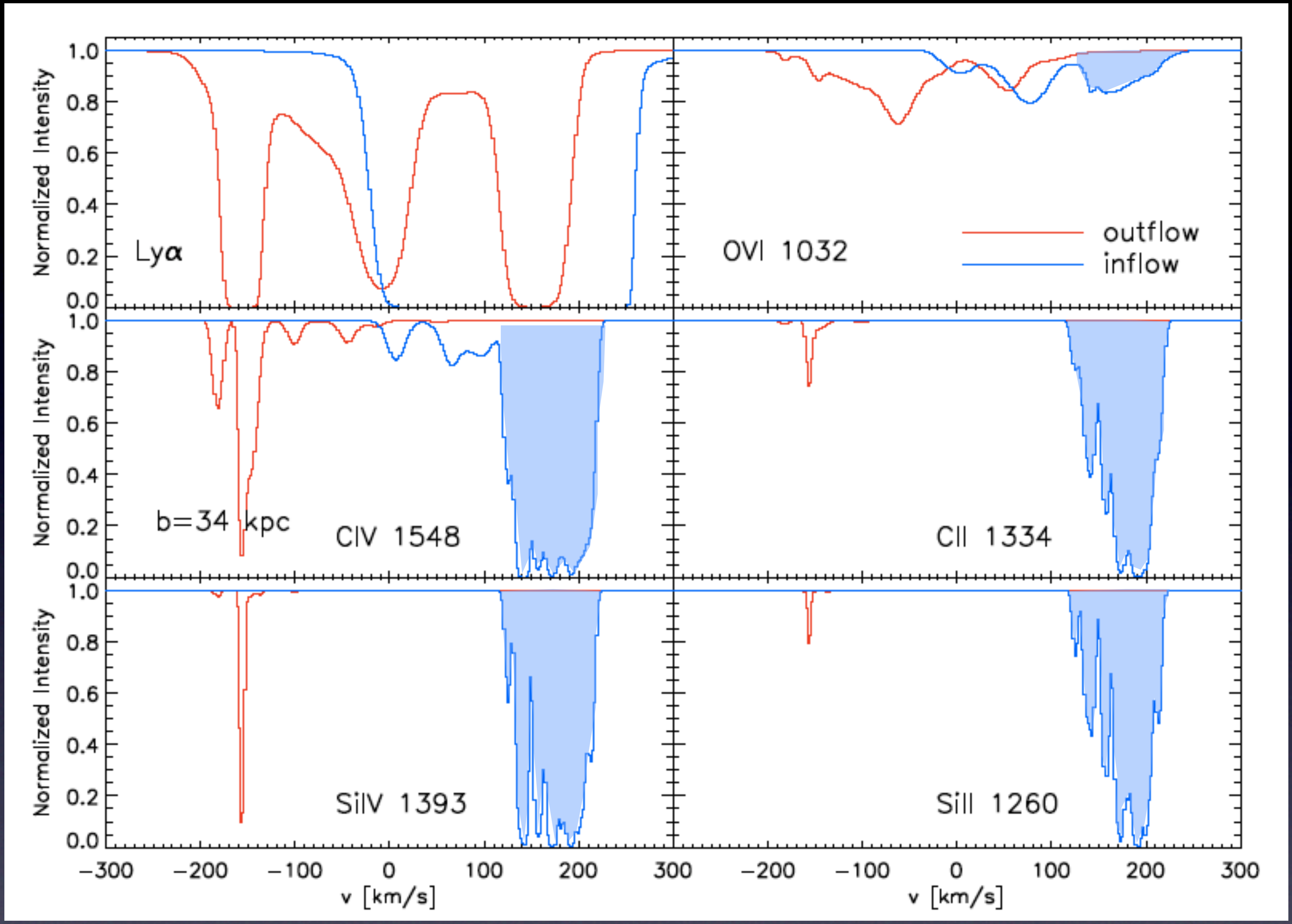

- Most, but not all, components exist in both high and low ions -- Multi-phase nature of absorbers
- Velocity range ~ ± 300 km/s

- Metal enriched infalling gas:
- $R_{vir} < r < 2R_{vir}$
- $\delta \sim 100$
- $Z > 0.03\ Z_{sun}$
- Enriched gas around nearby dwarf galaxy

- Optical depth $\tau(\nu) = \sum_j (m_j Z_j/m) W_{2D}(r_{jl}, h_j)\sigma_j(\nu)$; $\sigma_j(\nu)$ - cross section (Voigt function), $W_{2D}(r_{jl}, h_j)$ - 2D SPH kernel

- Rest frame equivalent width: $W_0 = c/\nu_0^2 \int [1-e^{-\tau(\nu)}]d\nu$

W_0-b Relation and Comparison with Observations

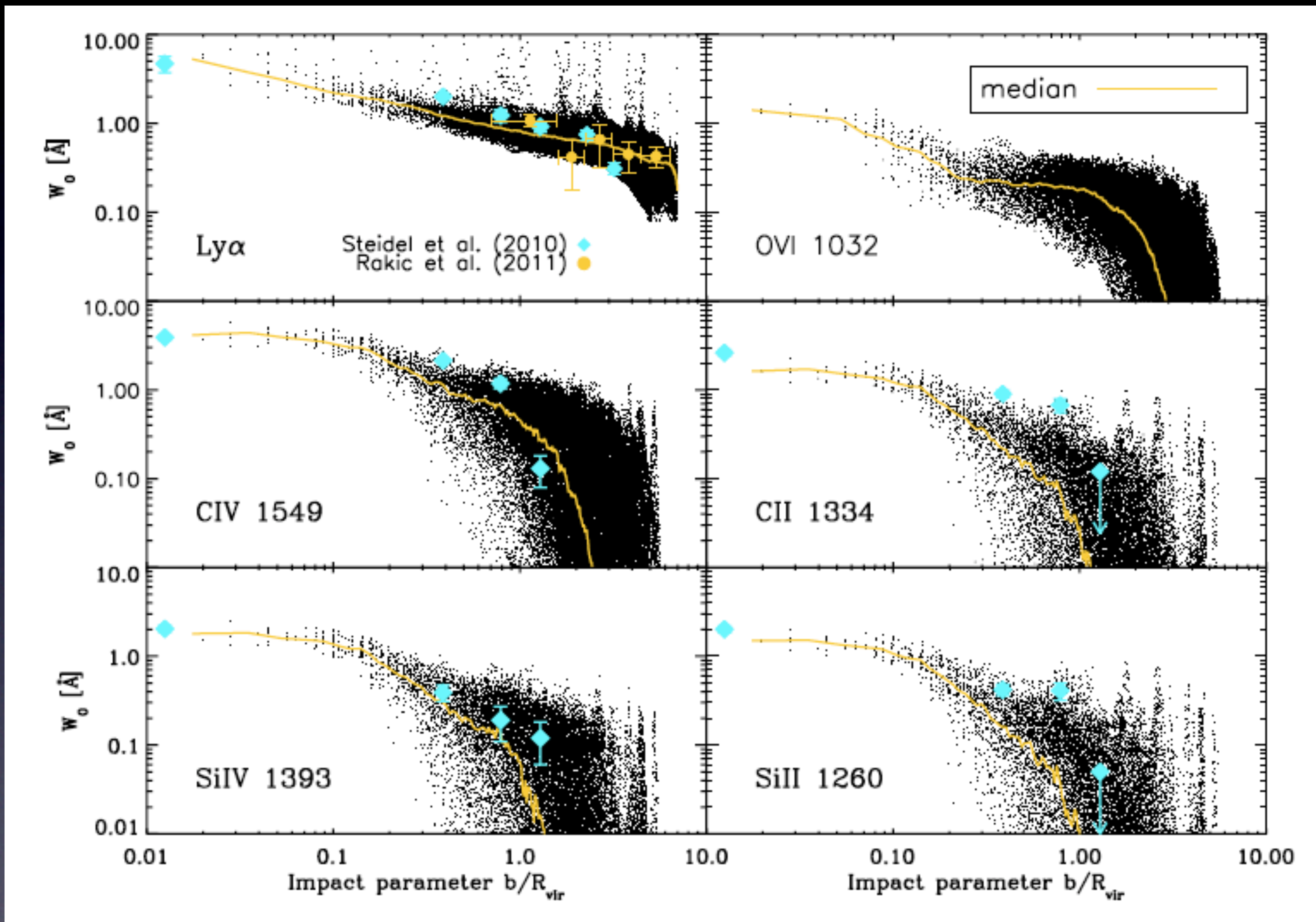

- Metal Line strength decline rapidly at 1-2 R_{vir}
- Line strength decline less fast for C IV, OVI and H I
- Ly α: remains strong to >~ 5 R_{vir}
- Broadly consistent with observations from Steidel+ (2010) and Rakic+ (2011)
- W_0 for metal ions: Higher than simulations without strong outflows (e.g., Fumagalli+ 2011; Goerdt + 2012)
- At small b, lines are mostly saturated -- W_0 determined by velocity

- 3 orthogonal projections, each has 500 x 500 evenly-spaced slightlines within b = 250 kpc region centered at the main host

W_0-b Relation and Comparison with Observations

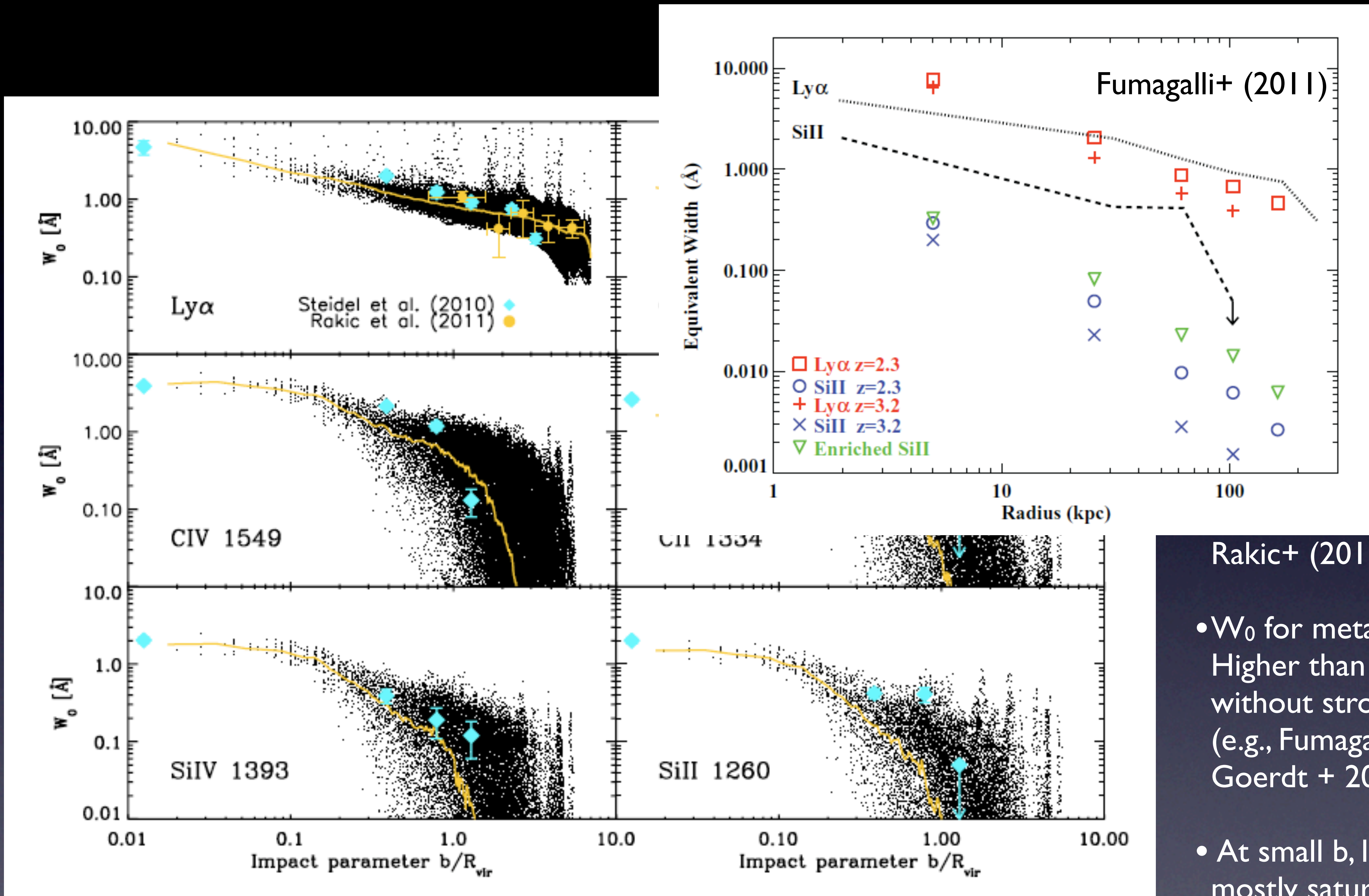

rength
ly at 1-2 R_{vir}

decline
C IV, OVI

s strong to

istent with
from
0) and
Rakic+ (2011)

- W_0 for metal ions: Higher than simulations without strong outflows (e.g., Fumagalli+ 2011; Goerdt + 2012)
- At small b, lines are mostly saturated -- W_0 determined by velocity

- 3 orthogonal projections, each has 500 x 500 evenly-spaced slightlines within b = 250 kpc region centered at the main host

Covering Factor of H I and Metal Ions

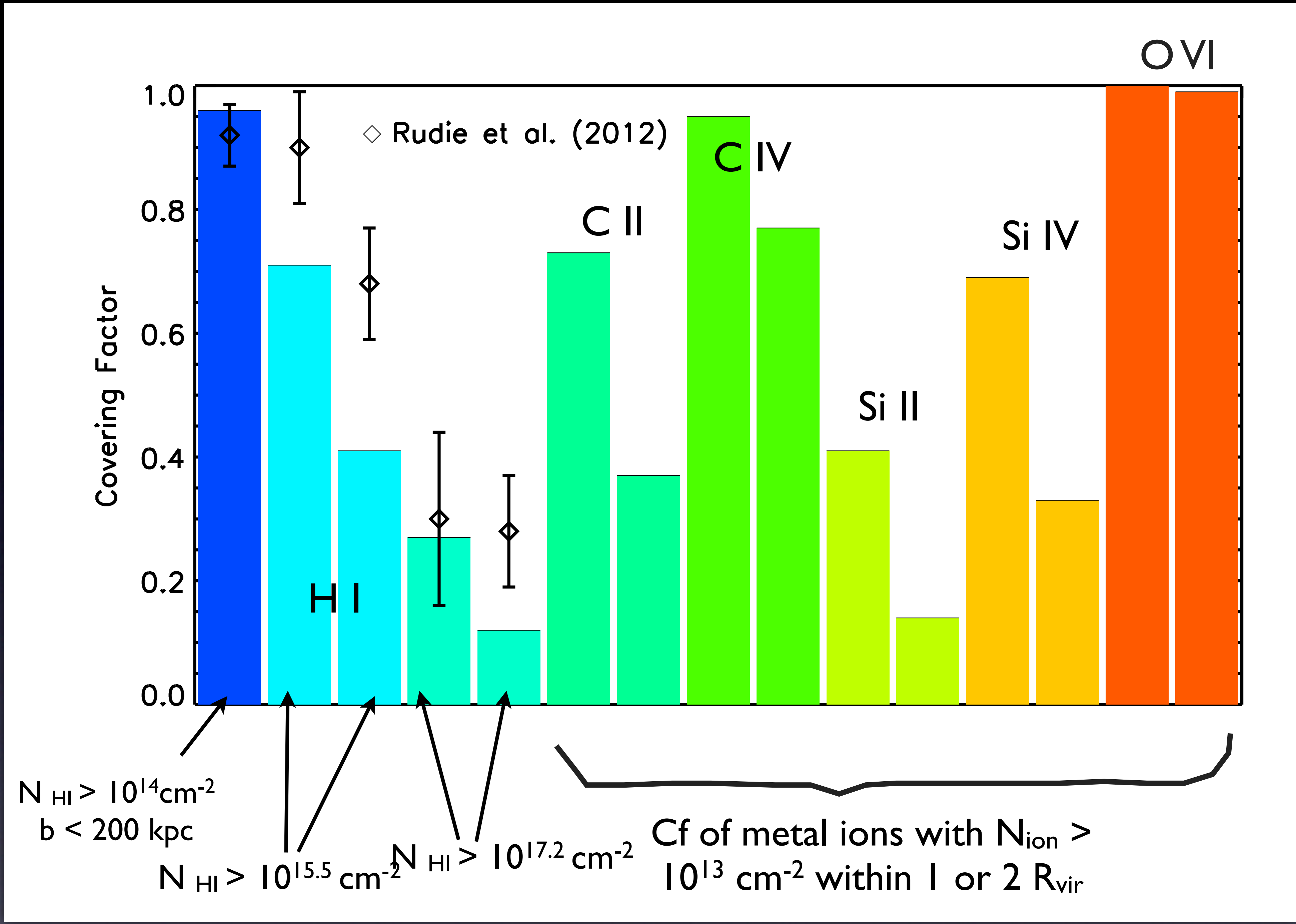

- O VI has covering factor (f_c) of unity in 2 R_{vir}. C IV also have large f_c
- C II, Si II, Si IV: smaller f_c, decline fast when $b > R_{vir}$

- In reasonable agreement with Rudie+ (2012) for H I, but in the low side
- HI covering factor: slightly higher, but comparable to simulations without strong outflows (e.g. Fumagalli+2011, Faucher-Giguère & Kereš 2011)

Detecting the Cold Streams: H I and Low Ions

- Cold ($T < 10^5$ K) inflow rates at R_{vir} $dM_{in,\,cold}/dt$ = 18 M_{sun}/yr, comparable to the SFR; $M_{in,\,hot}/dt \sim 5M_{sun}$/yr
- 35% inflow gas from nearby dwarfs
- Within 2 Rvir: 90% of LLS are inflowing gas, v_{in} <~ 150 -200 km/s

Detecting the Cold Streams: H I and Low Ions

Inflow only, optically thick gas

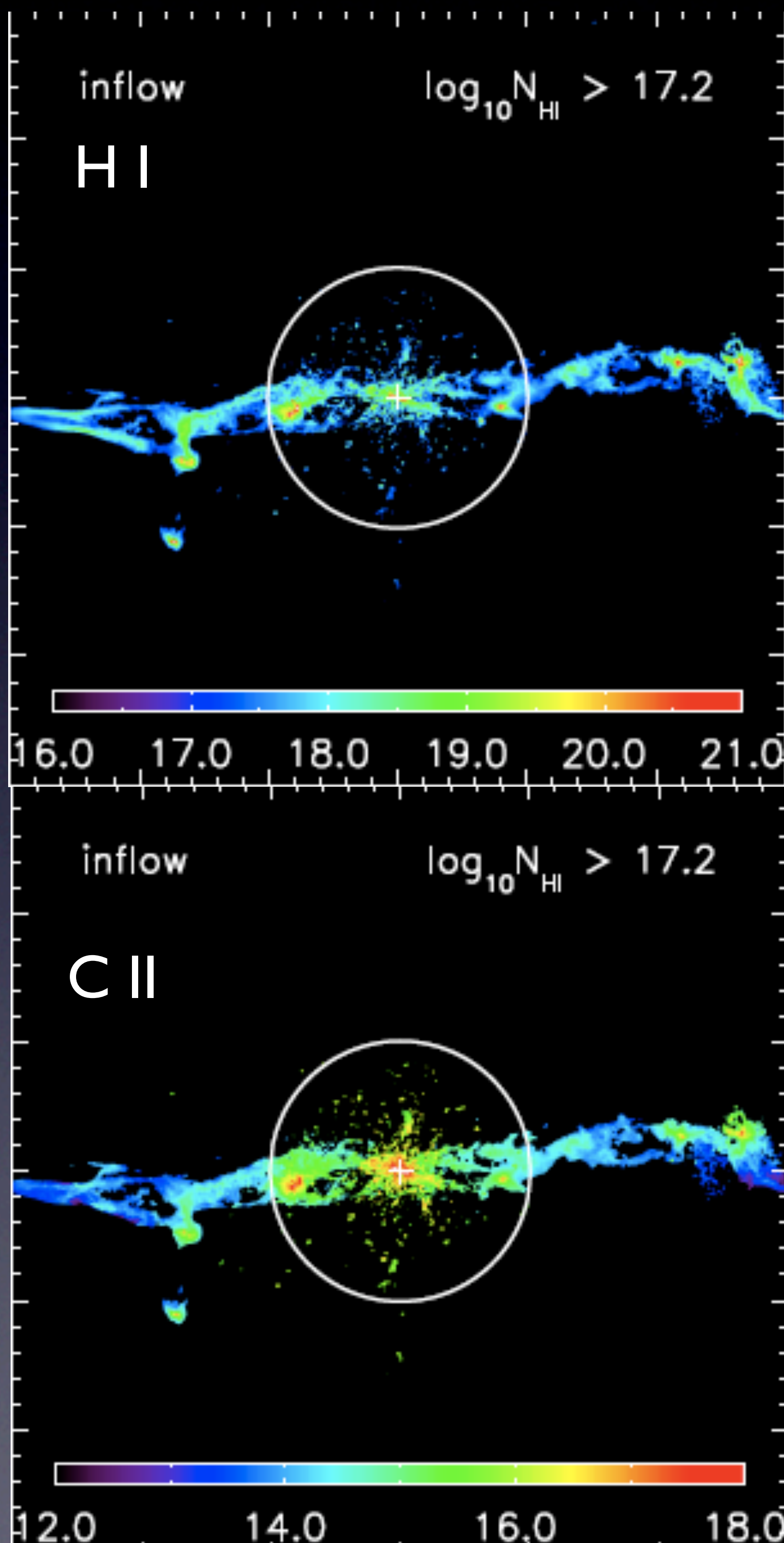

- Cold ($T < 10^5$ K) inflow rates at R_{vir} $dM_{in,\,cold}/dt$ = 18 M_{sun}/yr, comparable to the SFR; $M_{in,\,hot}/dt \sim 5 M_{sun}$/yr

- 35% inflow gas from nearby dwarfs

- Within 2 Rvir: 90% of LLS are inflowing gas, v_{in} <~ 150 -200 km/s

Detecting the Cold Streams: H I and Low Ions

Inflow only, optically thick gas

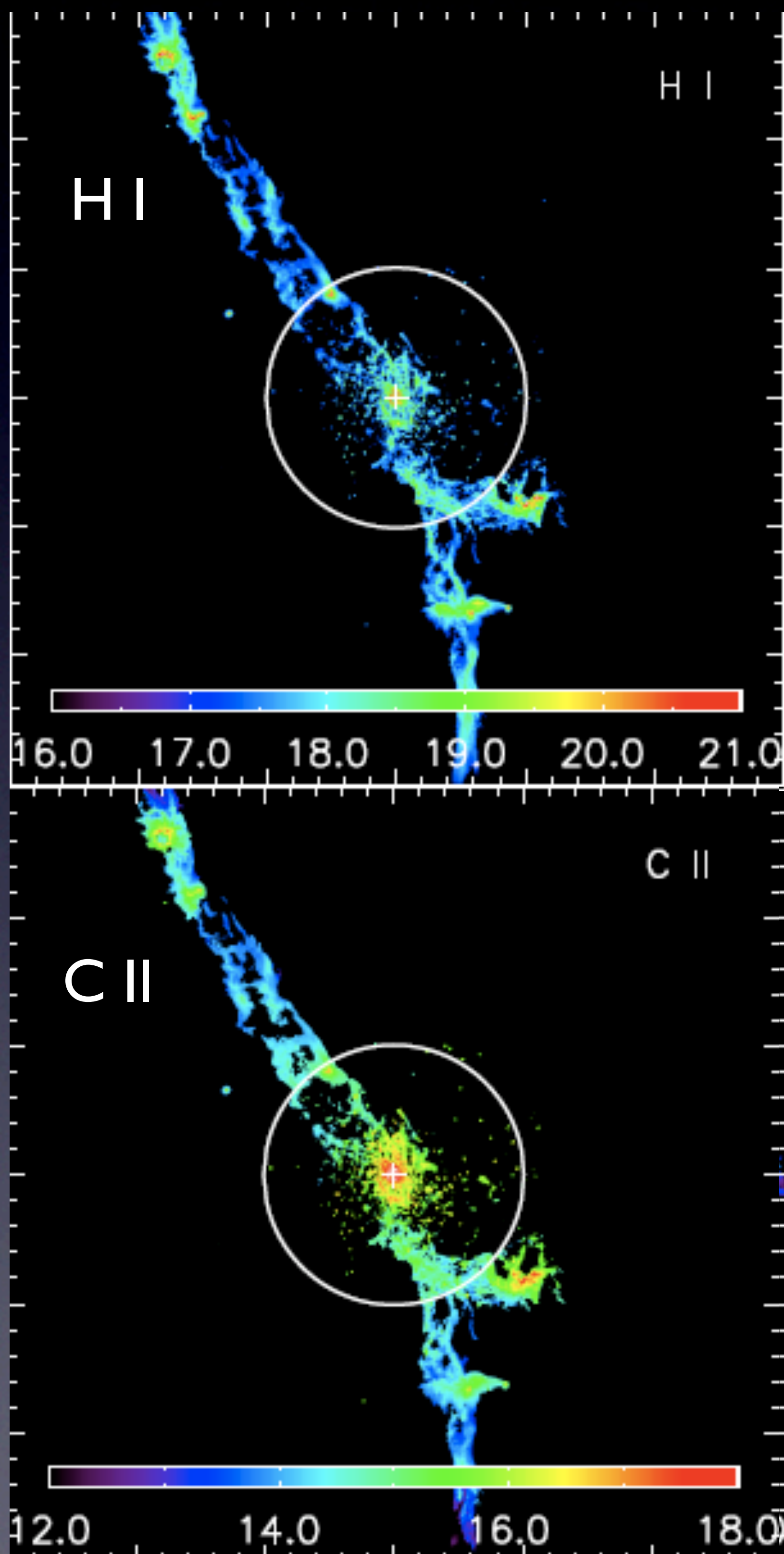

- Cold ($T < 10^5$ K) inflow rates at R_{vir} $dM_{in,\,cold}/dt$ = 18 M_{sun}/yr, comparable to the SFR; $M_{in,\,hot}/dt \sim 5 M_{sun}$/yr
- 35% inflow gas from nearby dwarfs
- Within 2 Rvir: 90% of LLS are inflowing gas, v_{in} <~ 150 -200 km/s

Detecting the Cold Streams: H I and Low Ions

Inflow only, optically thick gas

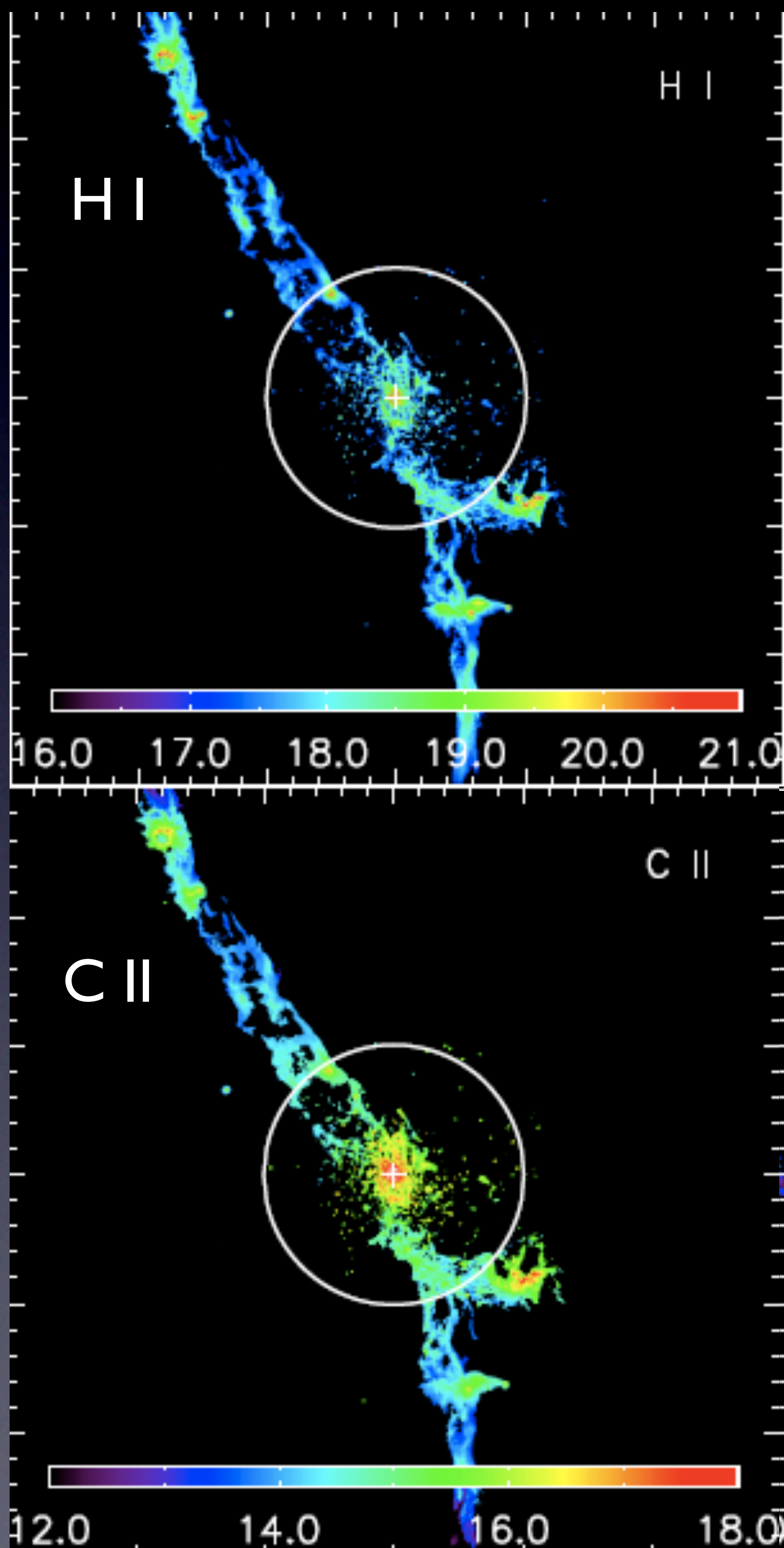

- Cold ($T < 10^5$ K) inflow rates at R_{vir} $dM_{in,\,cold}/dt$ = 18 M_{sun}/yr, comparable to the SFR; $M_{in,\,hot}/dt \sim 5 M_{sun}$/yr
- 35% inflow gas from nearby dwarfs
- Within 2 Rvir: 90% of LLS are inflowing gas, v_{in} <~ 150 -200 km/s
- Cold inflows are enriched: $Z_{LLS} > 0.03\ Z_{sun}$ for r < R_{vir}, and $Z_{LLS} > 0.01\ Z_{sun}$ within $2R_{vir}$
- Still lower than outflow metallicities Z_{out} = 0.1-0.5 Z_{sun}

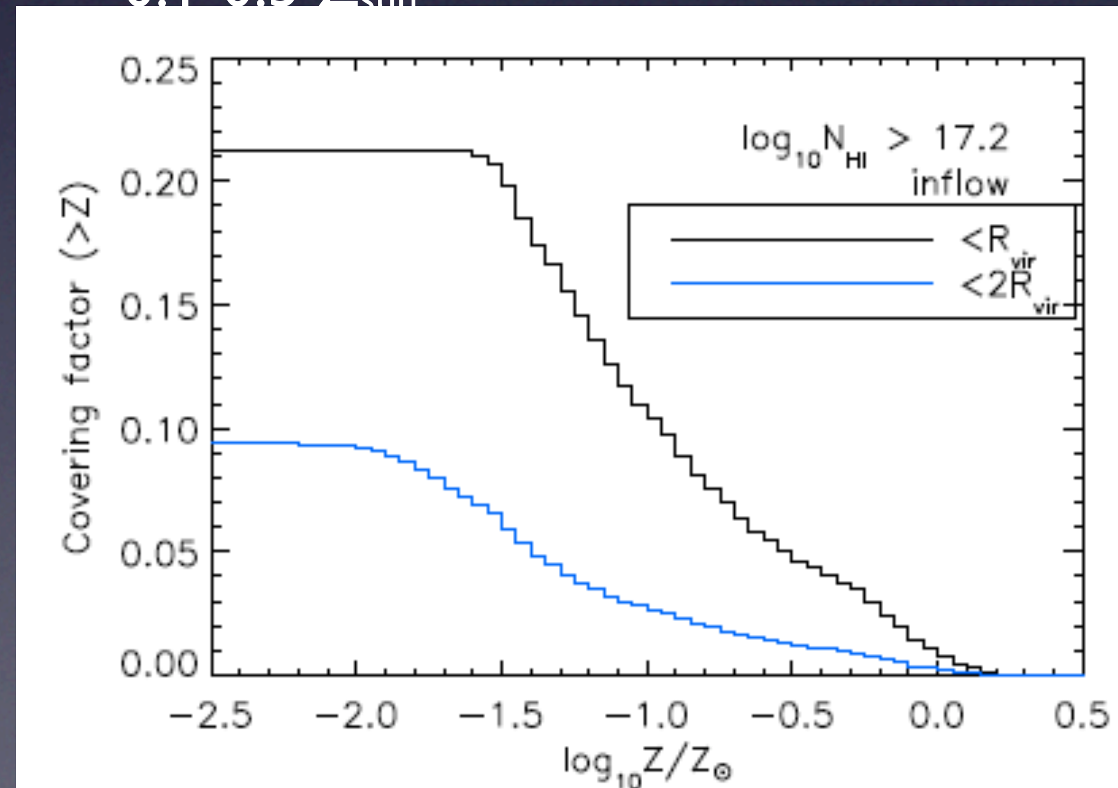

The N_{OVI}-b Relation in Eris2: Comparison with Low z Starburst Galaxies

- At z = 2.8, Eris2 has sSFR ~ 10^{-9} yr^{-1}, close to the local star burst galaxies in Tumlinson + (2011) and Prochaska+ (2011)
- N_{OVI}-b relation agreement with observations; but higher at b< 0.1 R_{vir}
- Typical N_{OVI} >~$10^{13\text{-}14}$ cm^{-2} up to 3 R_{vir}
- N_{OVI} -b mostly determined by SFR?

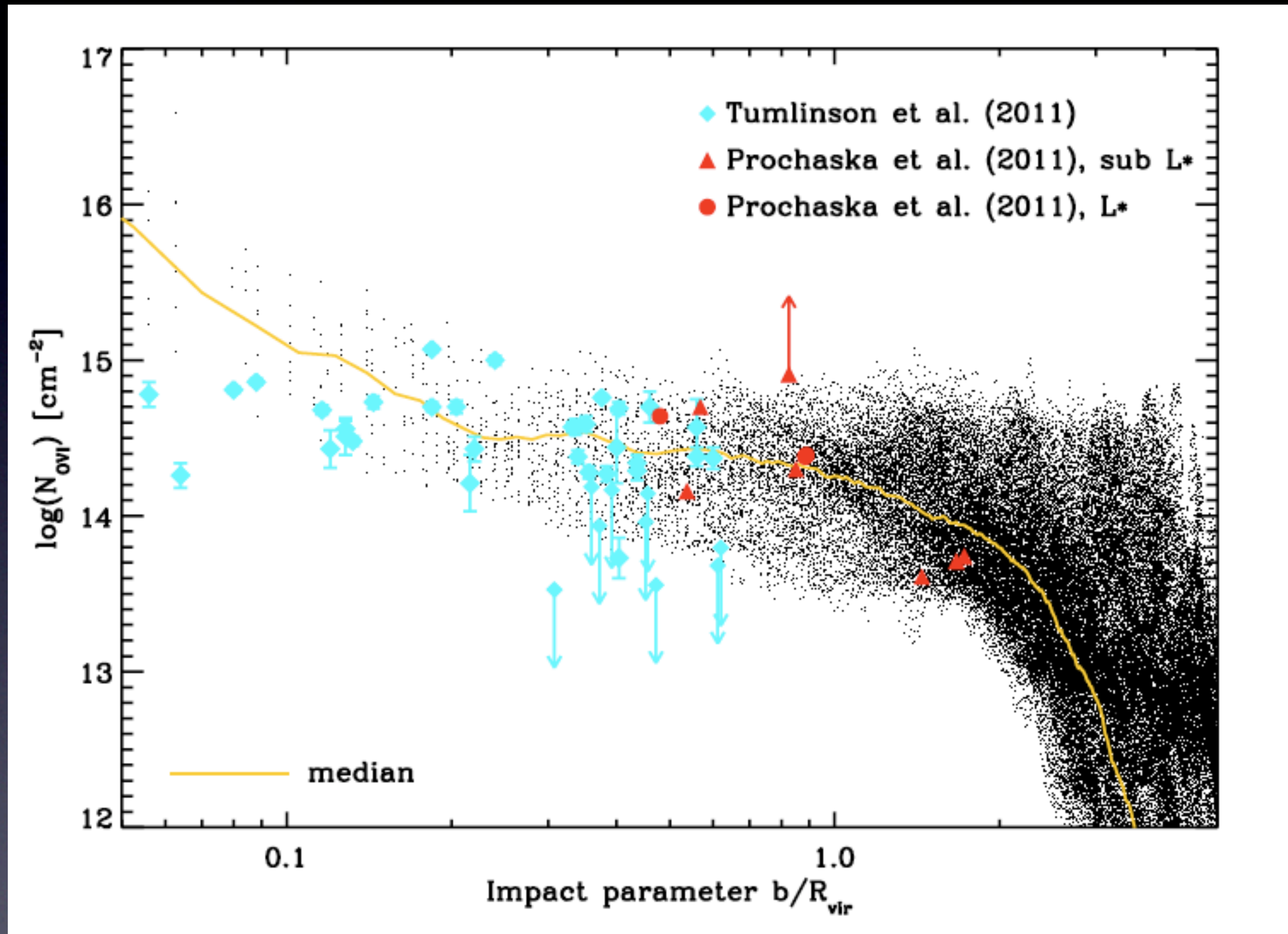

- R_{vir} ~ 160 kpc for sub-L* galaxies (Prochaska+ 2011)
- R_{vir} ~ 200-300 kpc for L* galaxies (Tumlinson+2011)

The Evolution of the CGM (Down to z=2.8)

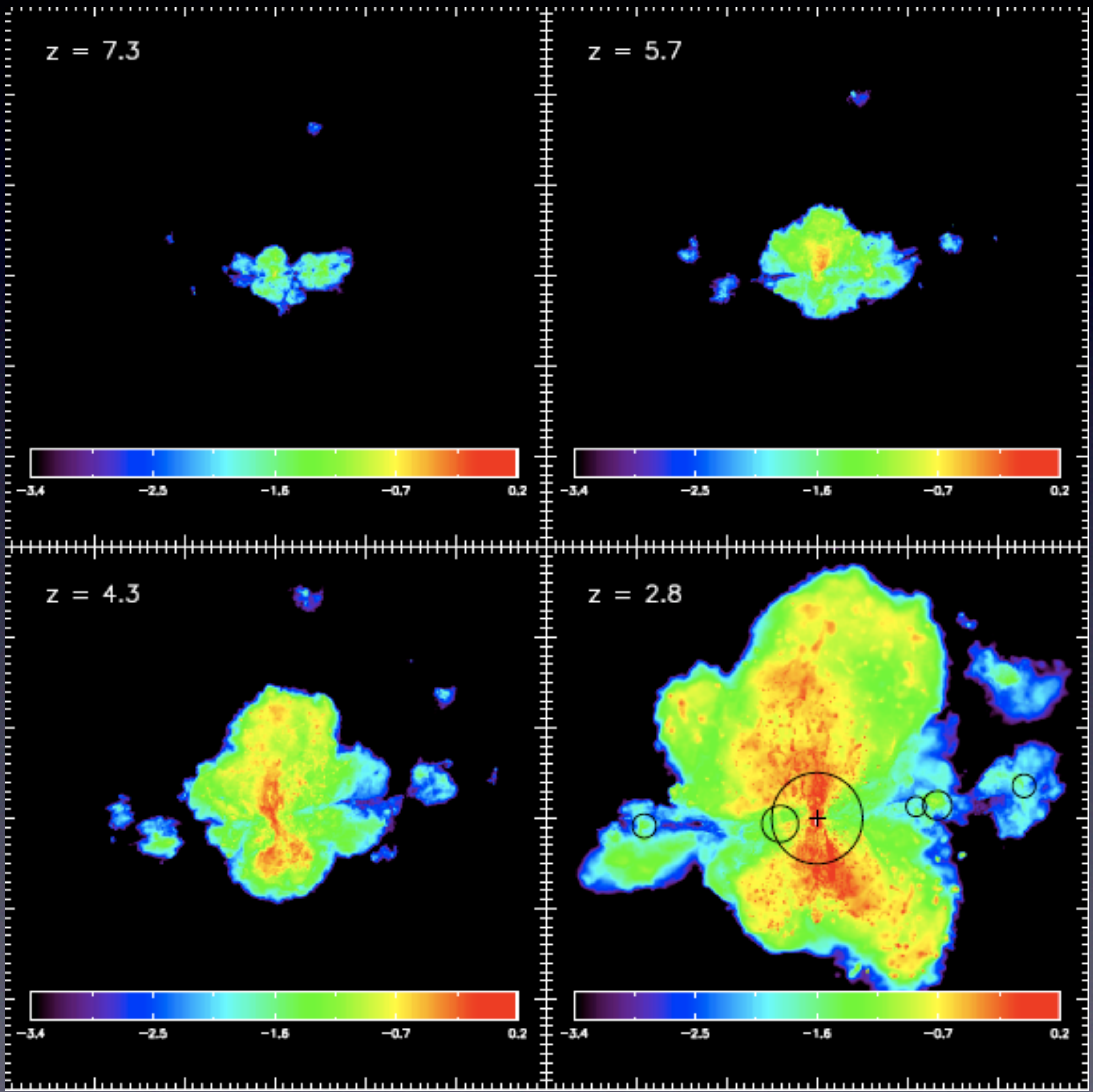

The Evolution of the CGM (Down to z=2.8)

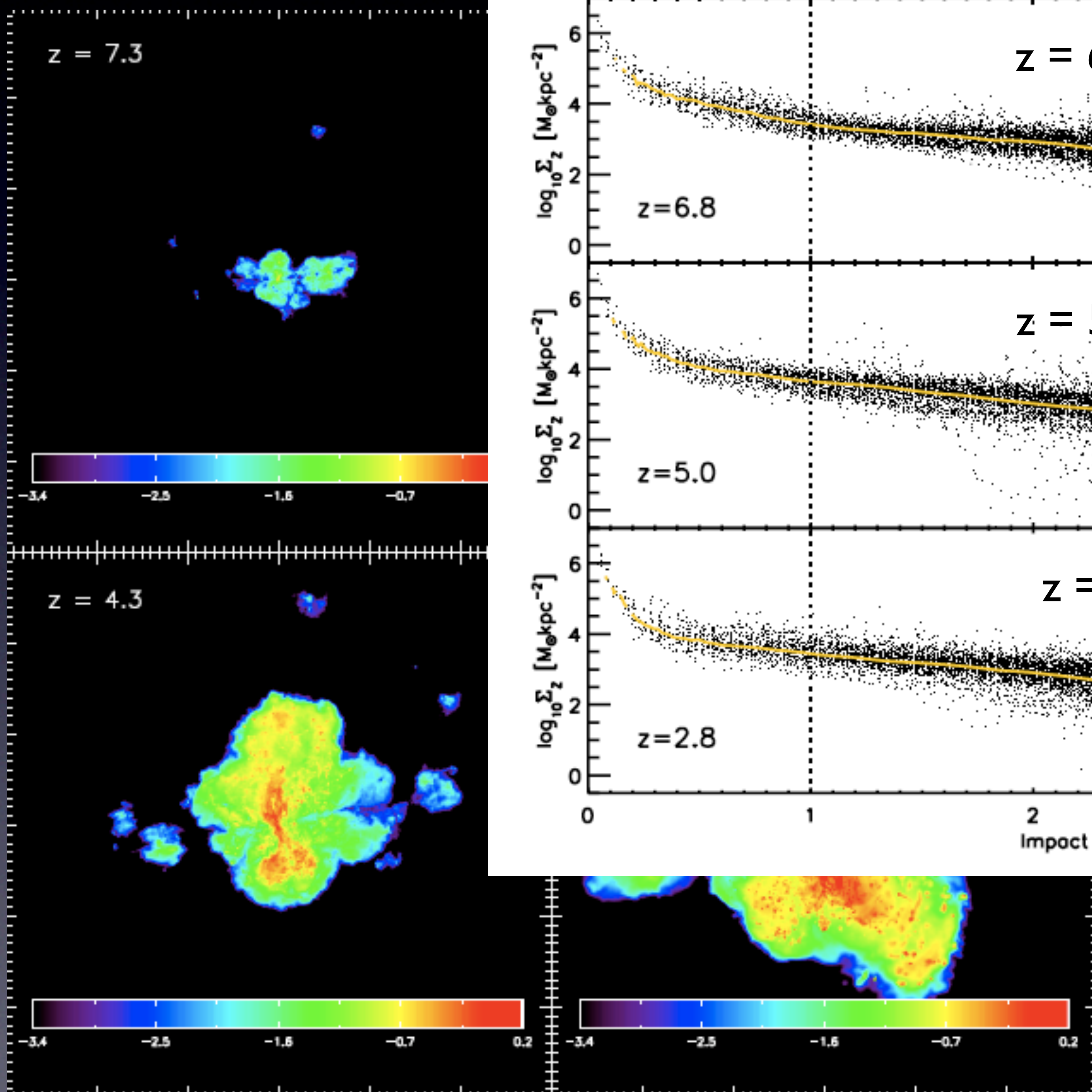

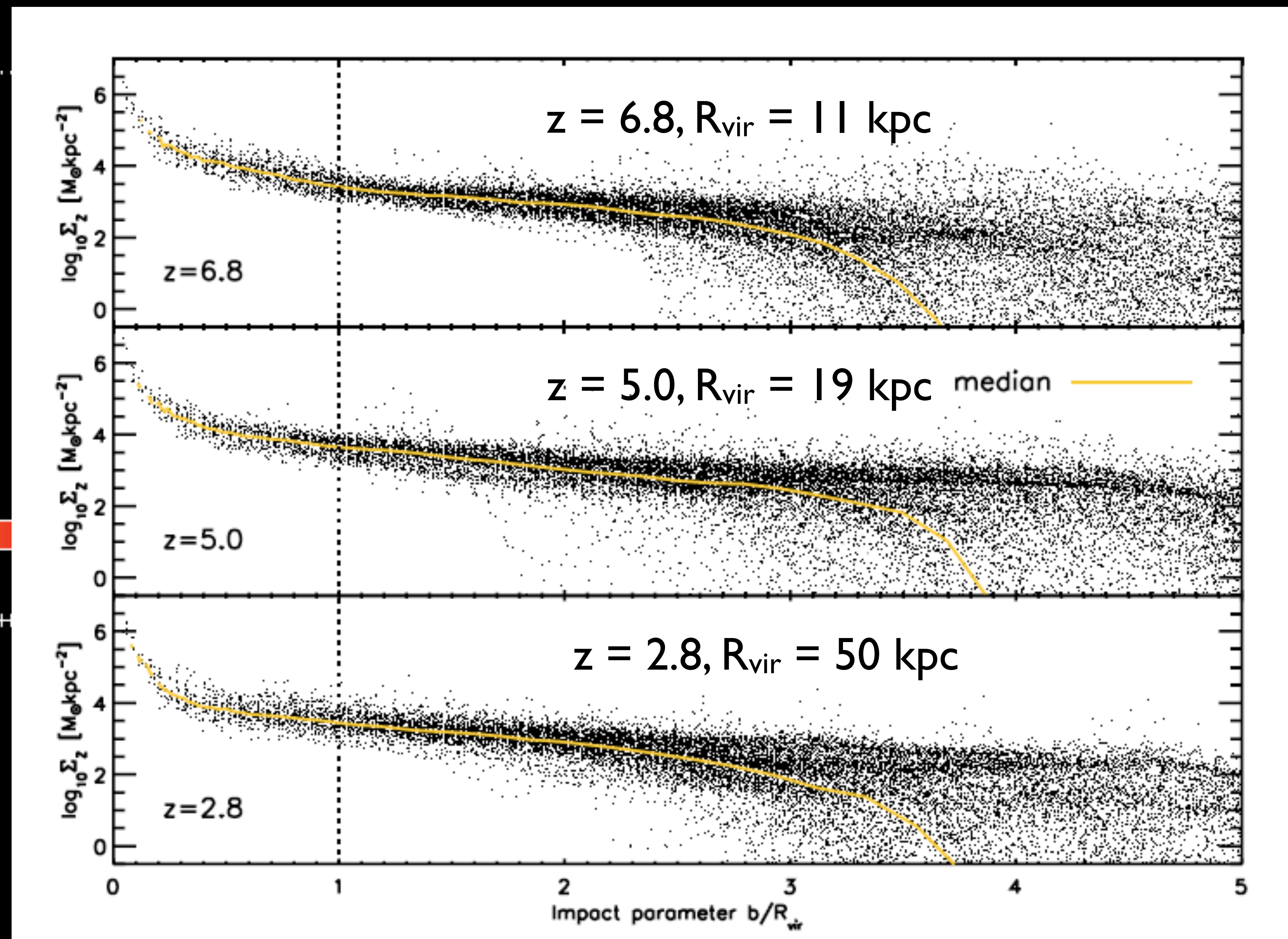

- From z = 8 to z ~ 3, the metal "bubble" scales well with R_{vir}
- z ~ 3 to z = 0?

The Effect of Gas Self-Shielding: W_0-b

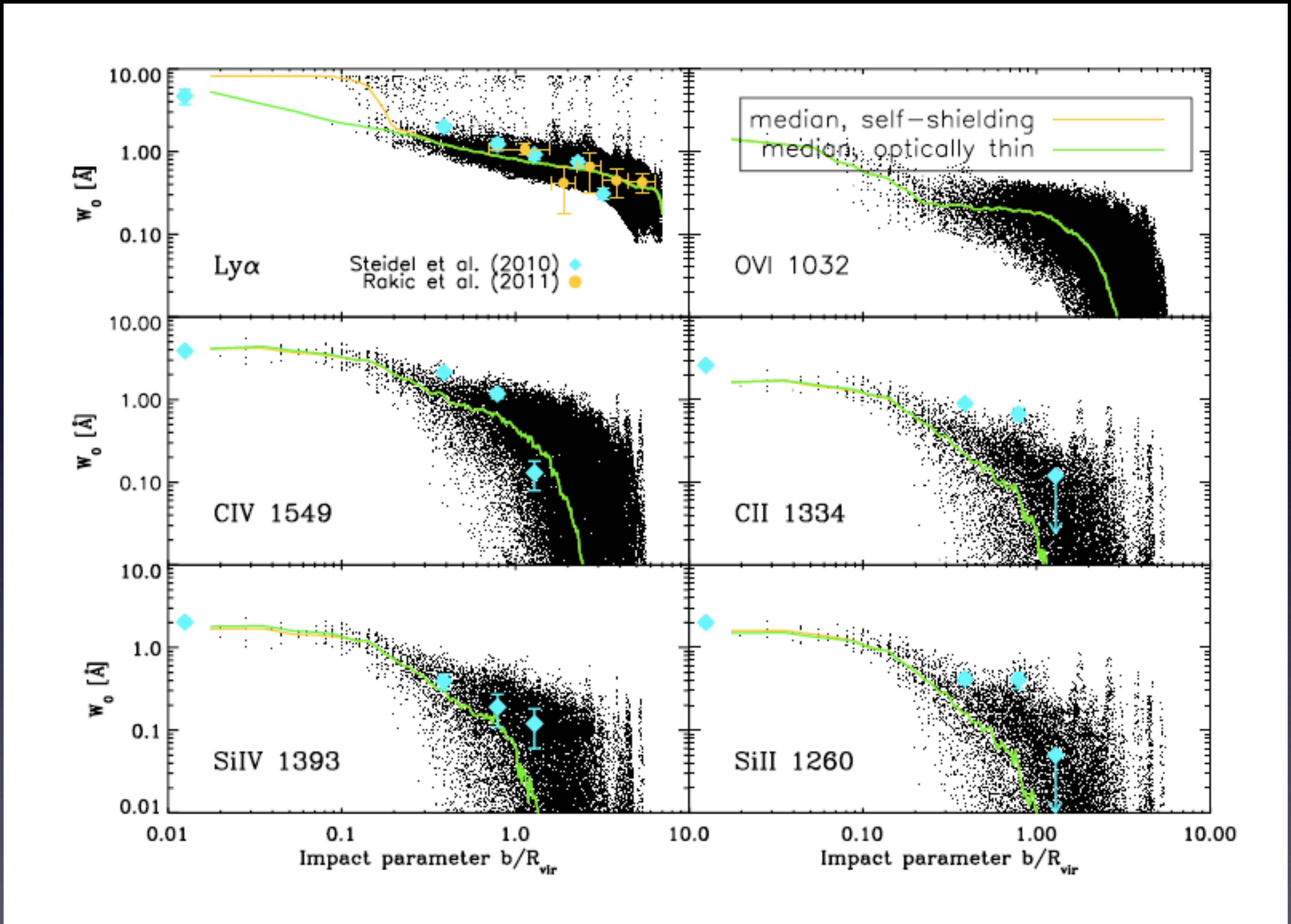

- Transition from optically thin to thick: $n_H \sim 0.01$ cm^{-3} (e.g. Fumagalli +2011; Goerdt +2012)
- Increase $N_{H\,I}$, $N_{Si\,II}$, decrease N_{CIV}, N_{CII}, N_{SiIV}
- OVI is not affected by much
- Metal lines: change in W_0 is not significant since lines are saturated

- Ly α: The data points within 10 kpc increases significant, W_0 become much higher than observations

The Effect of Metal and Thermal Diffusion - I

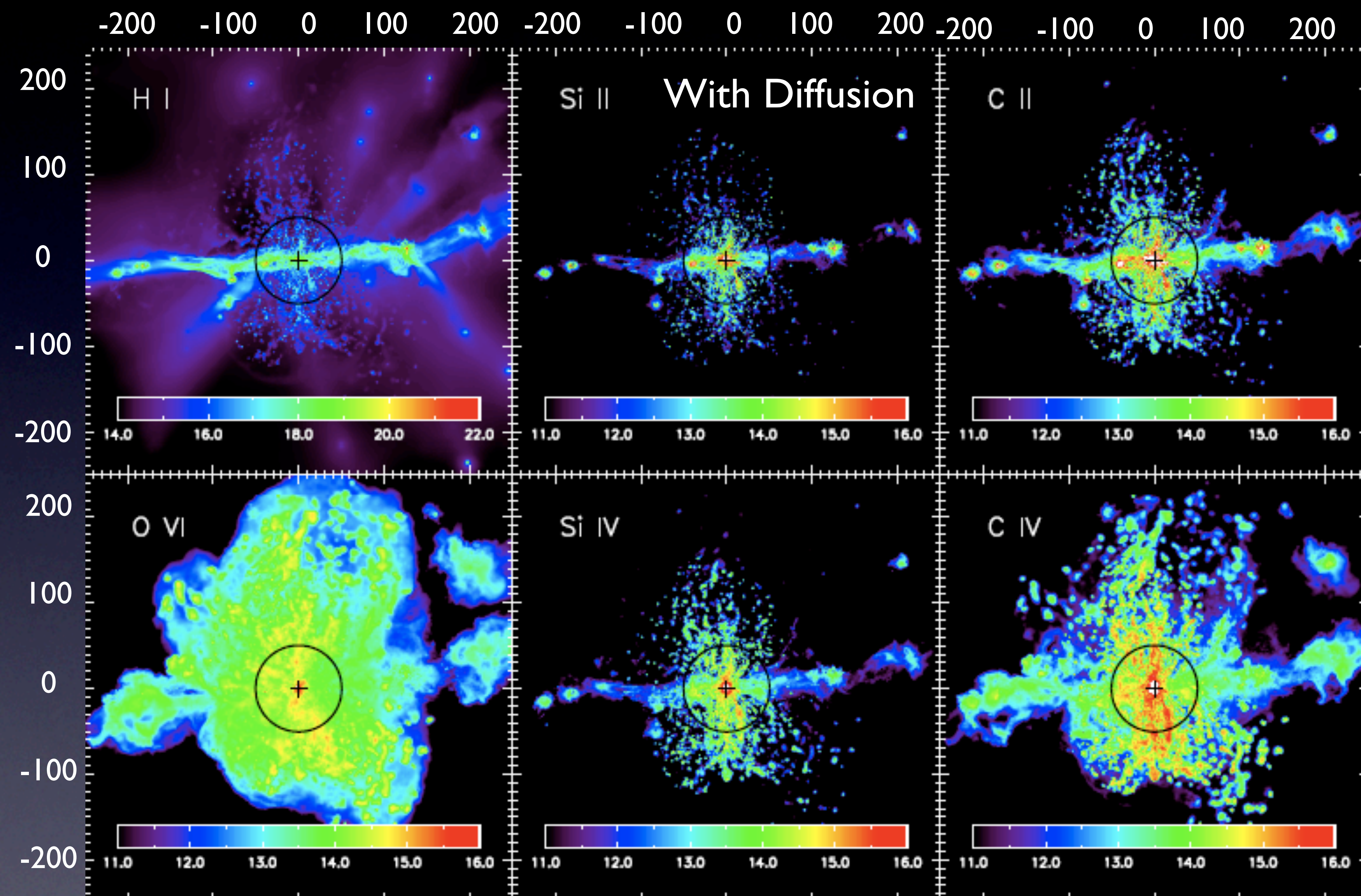

No turbulent mixing 1. Larger metal bubble (cf. Shen+ 2010);

2. "Clumpier" CGM due to higher Z and metal cooling;

3. Inflowing dwarfs are enriched, but less for the material in between

The Effect of Metal and Thermal Diffusion - I

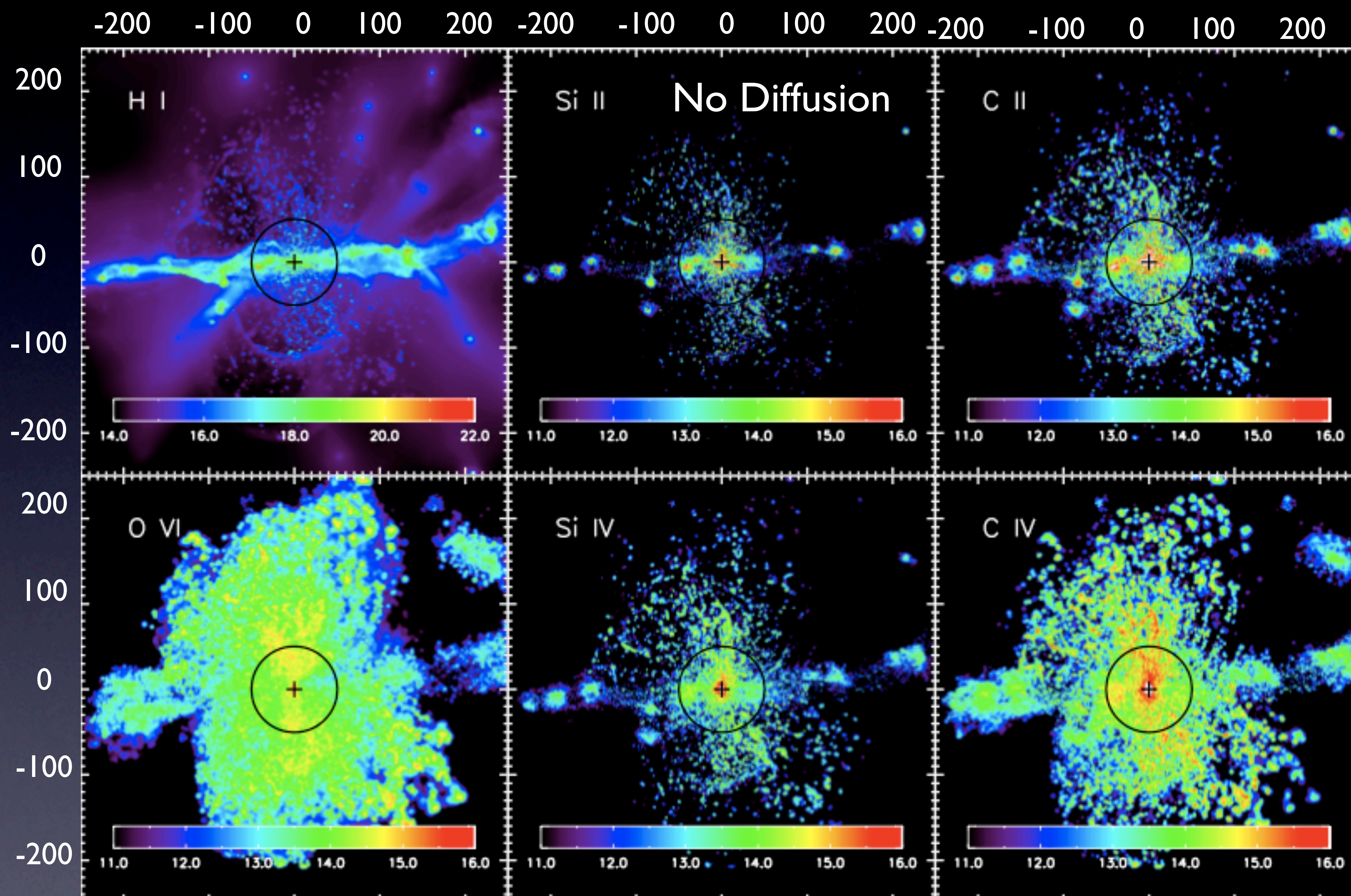

No turbulent mixing 1. Larger metal bubble (cf. Shen+ 2010);
2. "Clumpier" CGM due to higher Z and metal cooling;
3. Inflowing dwarfs are enriched, but less for the material in between

The Effect of Metal and Thermal Diffusion - II

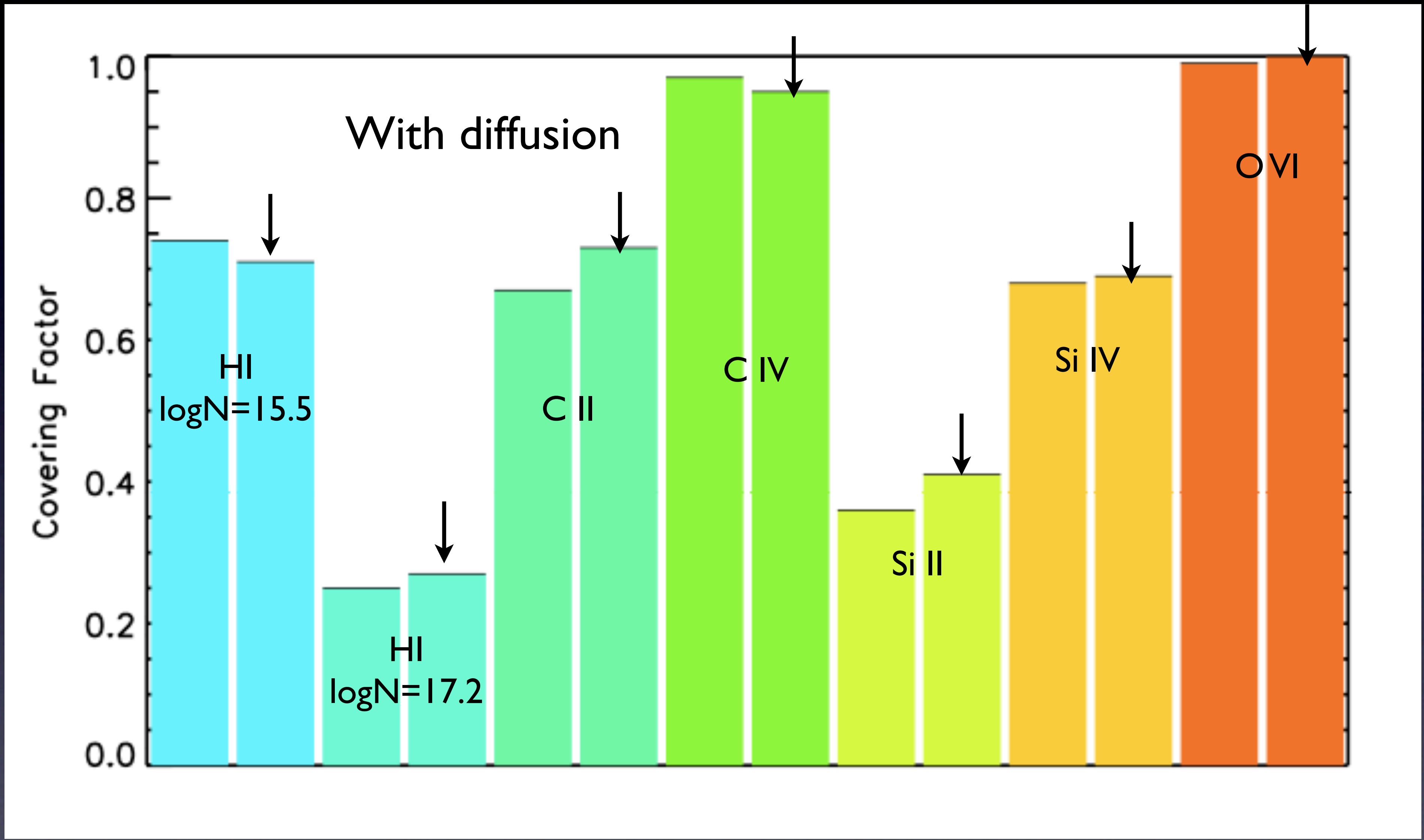

- The covering factor of metal ions at log N > 13 does not change significantly
- The covering factor of LLS H I, C II and Si II decreases because the CGM is clumpier
- CF for more diffuse H I and C IV increases because of more efficient wind

The Effect of Metal and Thermal Diffusion III

With Metal Diffusion

No Metal Diffusion

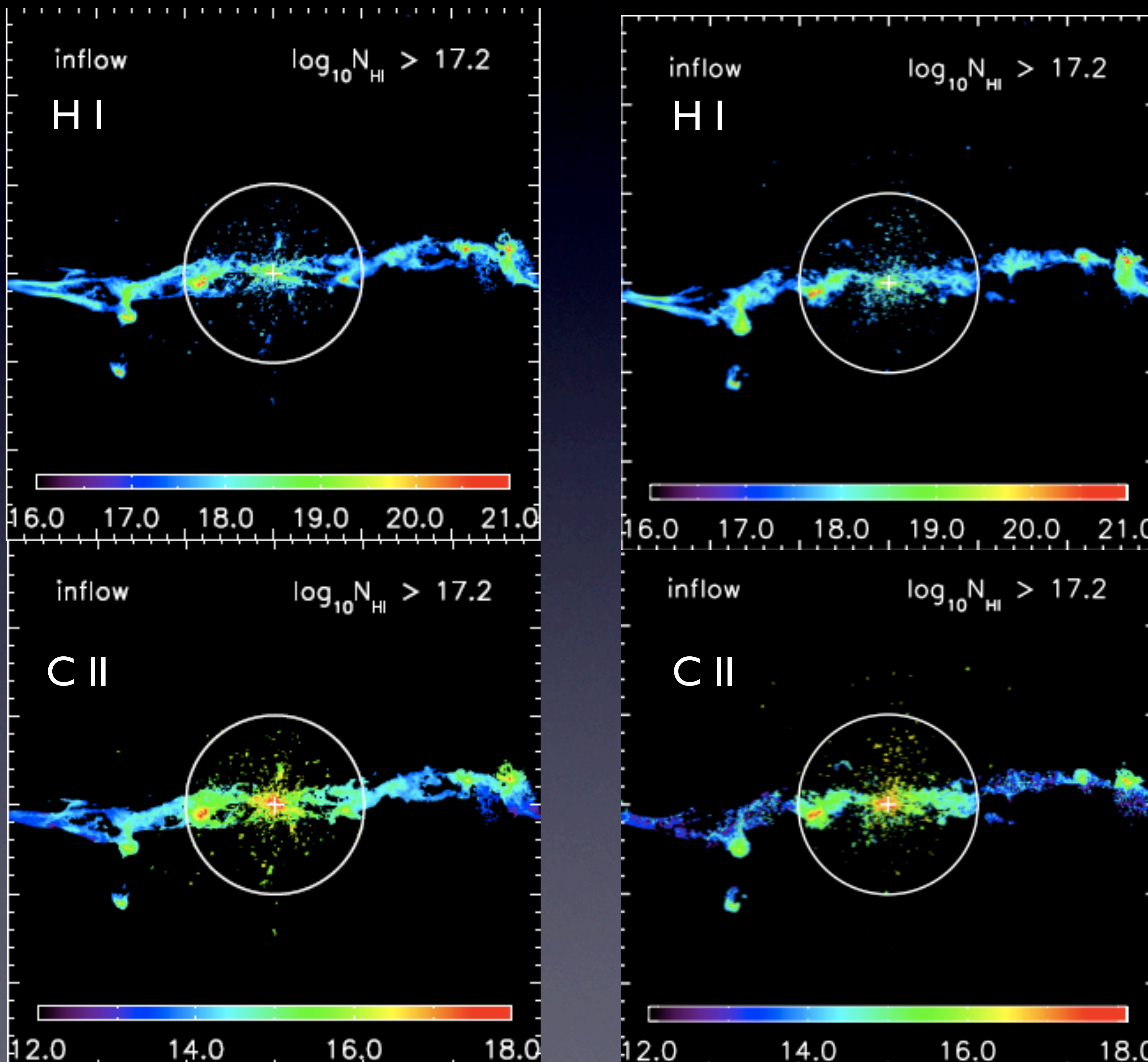

- Covering factor of both H I and low ions decreases

- Inflowing gas with N_{HI} > $10^{17.2}$ cm^{-2} and N_{CII} >10^{13} cm-2 decreases from 22% to 16% in R_{vir} and from 10% to 5% in 2R_{vir}

Effect of Metal Cooling on the CGM

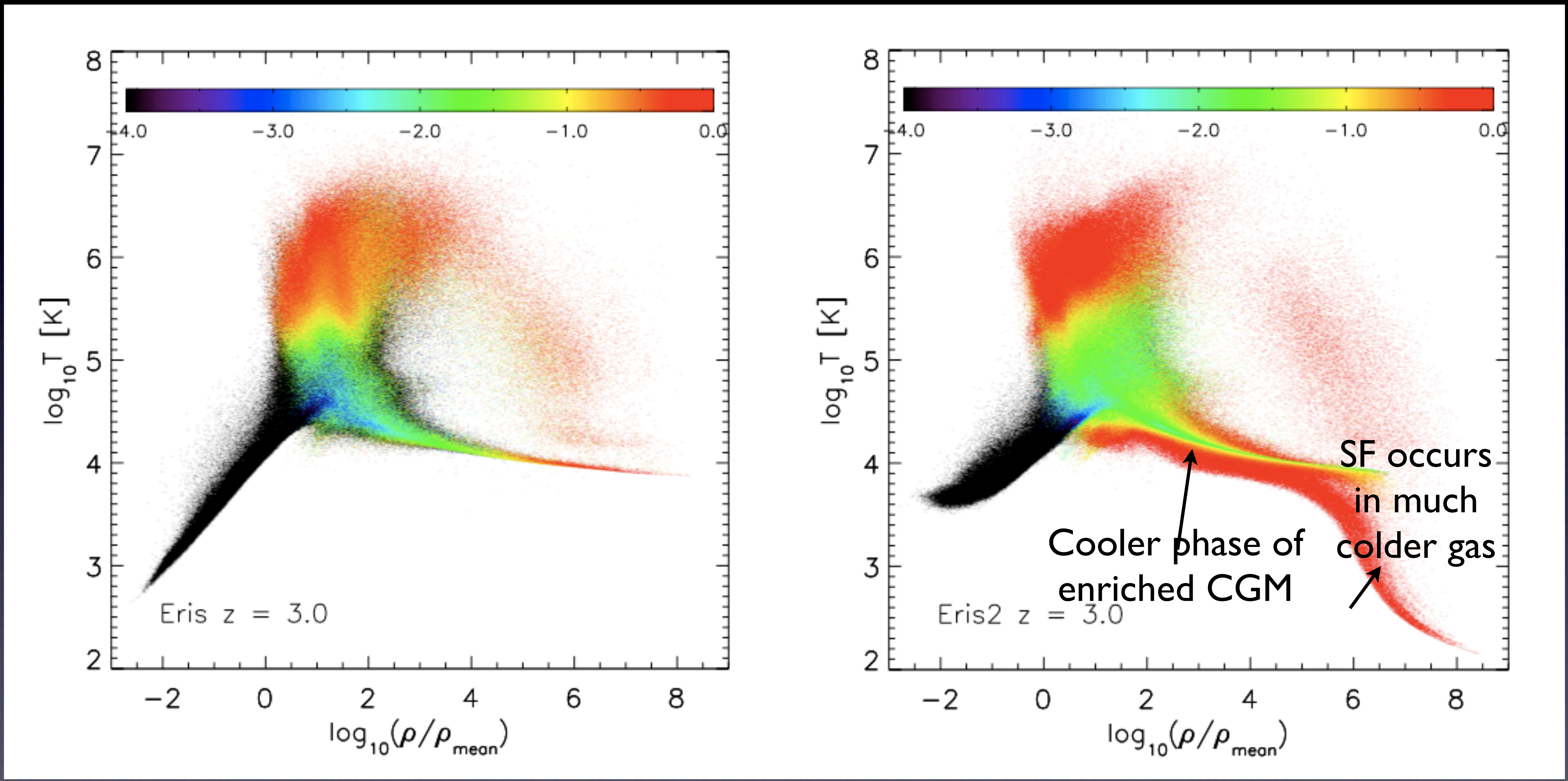

Distribution of Metals and Ions in ρ-T plane

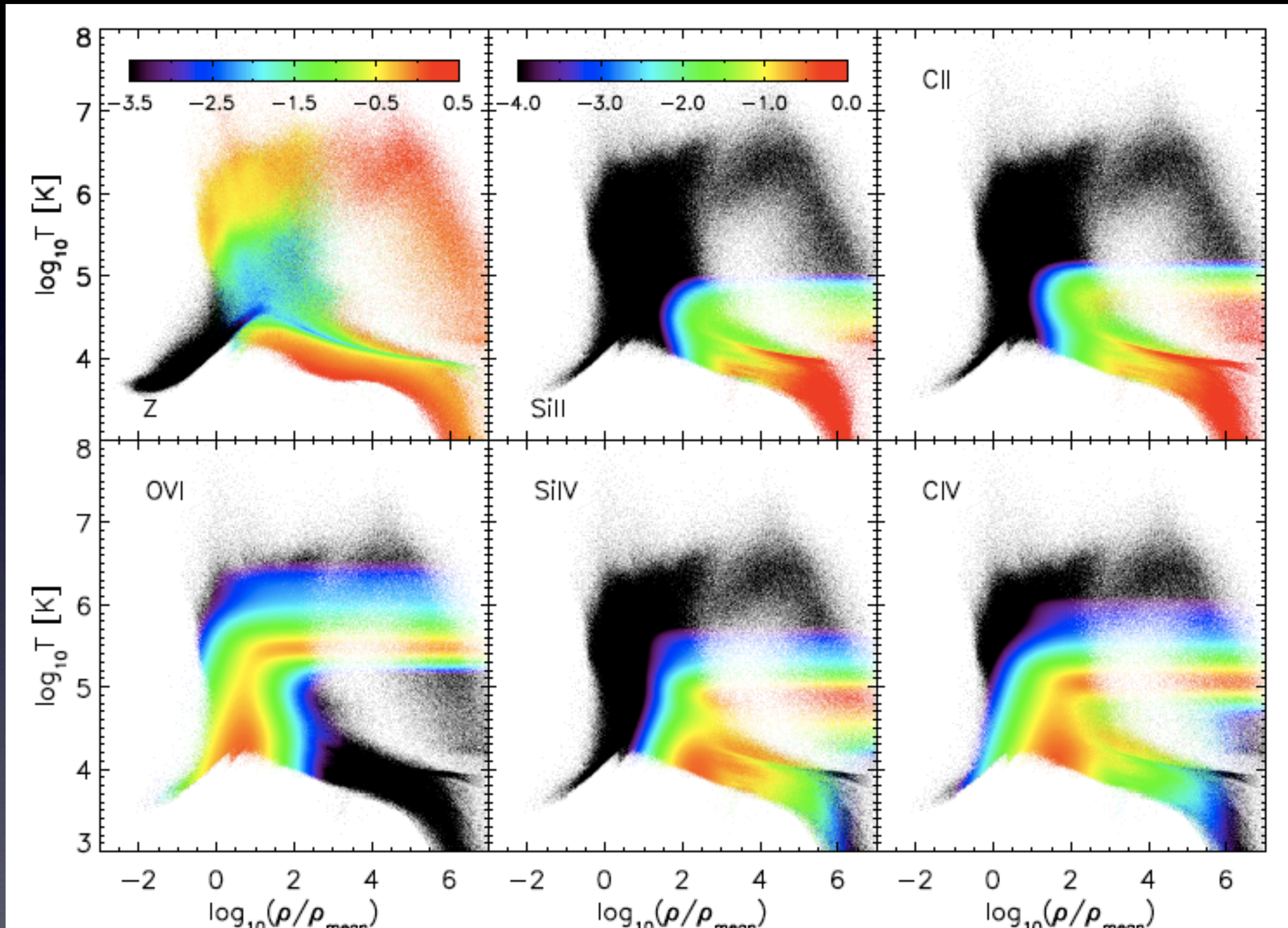

Summary

- Inflows and outflows coexist, about 1/3 of gas (by mass) within R_{vir} is outflowing, consistent with findings from cosmological simulations (e.g., van de Voort +2012);

- O VI absorbers have *both* collisional ionized and photoionized components, depending on distance. Large covering factor with typical $N_{OVI} > 10^{14}$ cm^{-2}, consistent with the data from local starbursts (Tumlinson+2011, Prochaska+2011) .

- Synthetic spectra shows inflows and outflows are multi-phase, although *not all* the O VI systems has corresponding low ion counterpart.

- W_0-b relation from Eris2 appears to be in reasonable agreement of observations of Steidel +(2010). Feedback & outflows are important, however inflowing material contributes significantly to the absorption line strength.

- The covering factor of LLS system is about 27% within Rvir, in good agreement with Rudie+ (2012), it is slightly higher than, but consistent with simulations with no strong outflows (Fumagalli+ 2011; Faucher-Giguère & Kereš 2011); 90% of LLS within 2R_{vir} are inflowing cold streams.

- The cold streams are enriched with CF of CII > 10^{13} about 22% within R_{vir} -- possible to detect inflows with metal line absorption.

- Metal mixing enhance the detection of cold flows using metals.

- Cooling due to metal lines are important for generating cooler phase of the CGM and possibly crucial for detection of the low ions.